Chapter 2
Mars in Short: Past and Present Geology and Climate

Sandra Siljeström, Sarah Baatout, Jean-Pierre de Vera, Veronique Dehant, Caroline Freissinet, Christoph Gross, Natuschka M. Lee, Nicolas Mangold, Lena Noack, Ana-Catalina Plesa, Attilio Rivoldini, and Inge Loes ten Kate

S. Siljeström (✉)
RISE Research Institutes of Sweden, Stockholm, Sweden
e-mail: sandra.siljestrom@ri.se

S. Baatout
Belgian Nuclear Research Center, Mol, Belgium
e-mail: sbaatout@sckcen.be

J.-P. de Vera · A.-C. Plesa
German Aerospace Center (DLR), Köln, Germany
e-mail: jean-pierre.devera@dlr.de; ana.plesa@dlr.de

V. Dehant
Royal Observatory of Belgium and UC Louvain, Brussels, Belgium
e-mail: veronique.dehant@oma.be

C. Freissinet
CNRS, St Quentin en Yvelines, France
e-mail: caroline.freissinet@latmos.ipsl.fr

C. Gross · L. Noack
Freie Universität Berlin, Berlin, Germany
e-mail: christoph.gross@fu-berlin.de; lena.noack@fu-berlin.de

N. M. Lee
Swedish Collegium for Advanced Study and Swedish University of Agricultural Sciences, Uppsala, Sweden
e-mail: natuschka.lee@slu.se

N. Mangold
LPG, CNRS, Université de Nantes, Nantes, France
e-mail: nicolas.mangold@univ-nantes.fr

A. Rivoldini
Royal Observatory of Belgium, Brussels, Belgium
e-mail: rivoldini@oma.be

I. L. ten Kate
Utrecht University and University of Amsterdam, Utrecht, the Netherlands
e-mail: i.l.tenkate@uu.nl

C. Verseux et al. (eds.), *Mars and the Earthlings: A Realistic View on Mars Exploration and Settlement*, Space and Society,
https://doi.org/10.1007/978-3-031-66881-4_2

Table 2.1 Basic parameters about Mars

Parameter	Facts about Mars
Radius (Equatorial)	≈ 53% of Earth (3396 km vs 6380 km)
Volume	≈ 15% of the Earth
Mass	≈ 11% of the Earth
Surface gravity	≈ 38% of the Earths (3.71 m/s^2 vs 9.81 m/s^2)
Solar day duration (sol)	≈ 24 h 40 min (102% of the Earth)
Solar year duration	≈ 687 days
Solar influx	Between 37% and 50% of the earth
Distance to the Sun (mean)	1.52 times Earth distance to the sun; 230 million km vs 150 million km
Seasons	Twice as long as on the Earth
Moons	Phobos ø≈ 22 km and Deimos ø≈ 12 km
Temperature	From −143 °C to +27 °C
Magnetic field	No global magnetic field
Climate/radiation	Extreme/hazardous

Mars is easily observed in the sky due to its reddish colour and has therefore been the target of inspiration since the early history of mankind. It is the second smallest planet in the Solar System (diameter: ca. 6790 km), and the fourth and farthest terrestrial planet from the Sun (230 million km). Mars differs from Earth regarding several parameters (Table 2.1).

Mars has been exposed to dramatic geological processes throughout its history. Today, the surface of Mars is characterized by extreme contrasts, such as the Martian dichotomy between the northern and the southern hemisphere, huge canyons, and some of the highest volcanoes in the Solar system (Fig. 2.1). The first map of the surface of Mars was drawn in 1840 by Johann Heinrich von Mädler. Since then, many improvements have been made, based on data from space missions to Mars. Now Mars has become the target of what may become one of mankind's most advanced technical and scientific endeavours: the first human mission to another planet in the Solar System. Knowledge about its present and past geology and environment is crucial for this endeavour and our understanding of how Mars was formed, how it developed throughout time, whether a form of life has ever existed on Mars.

2.1 Geological History of Mars

Mars was formed at the same time as the other terrestrial planets in the Solar System, approximately 4.6 billion years ago. Its geological history can be divided into different periods (Fig. 2.2).

Pre-Noachian period (4.5–4.1 billion years-Gyr-ago). Little is known about the first period of Martian history, dating back to the formation of the crust, about

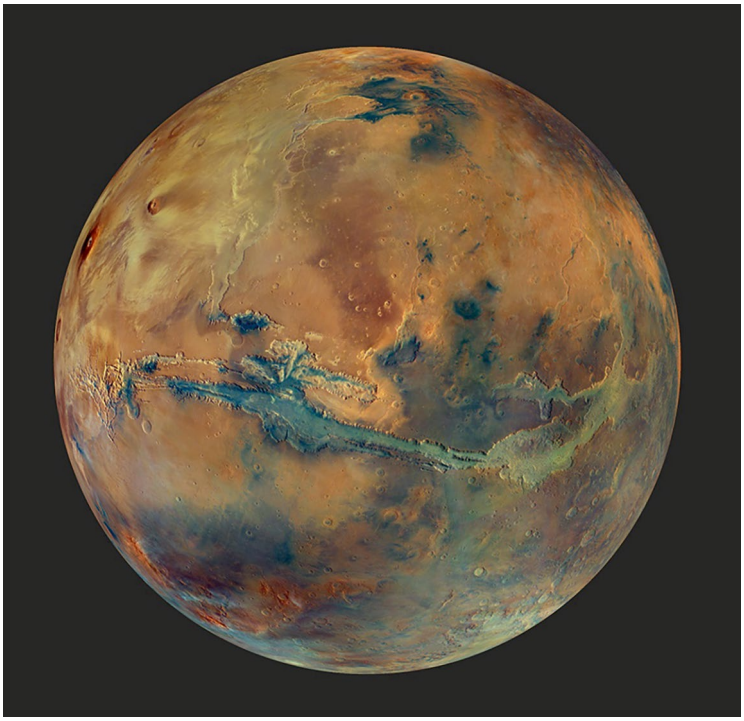

Fig. 2.1 Mars colour mosaic produced by the High-Resolution Stereo Camera team, simulating a view from 2500 km above Valles Marineris, with locally enhanced colour and contrast (Image credit: ESA/DLR/FU Berlin/https://doi.org/10.17169/refubium-40624 and https://doi.org/10.57780/esa-t4y39mj)

4.5 Gyr ago. This period was a chaotic time with an ongoing heavy bombardment and colossal basin-forming impact events, which was then presumably followed by a 400-million-year (Myr) hiatus, until the next bombardment started (Bottke & Andrews-Hanna, 2017; Burt et al., 2008). *In situ* calibration of the cratering-chronology models with cosmogenic and radiogenic isotope ages, obtained by NASA's Curiosity rover, suggests a monotonic flux decay since between 4.45 and 4.24 Gyr (Werner, 2019). During this period, the largest lowlands on Mars, the Vastitas Borealis region, which encircles the northern polar region, were formed. Presumably, Mars had initially a very dense atmosphere, resulting from impacts and mantle outgassing. Large parts of its surface, such as the Noachian Highlands, were covered with water ('NASA Astrobiology', 2023; Rodriguez et al., 2020).

Crucially, however, during this period the Sun shone less brightly than it does today (by approximately 30%). Considering that Mars is further away from our star than the Earth, its atmosphere would have had to provide strong greenhouse forcing for large bodies of water not to have been frozen at their surface. It is nevertheless likely that substantial internal heat would have resulted in a liquid water layer, in contact with the surface, that was capable of flowing and carving channel systems.

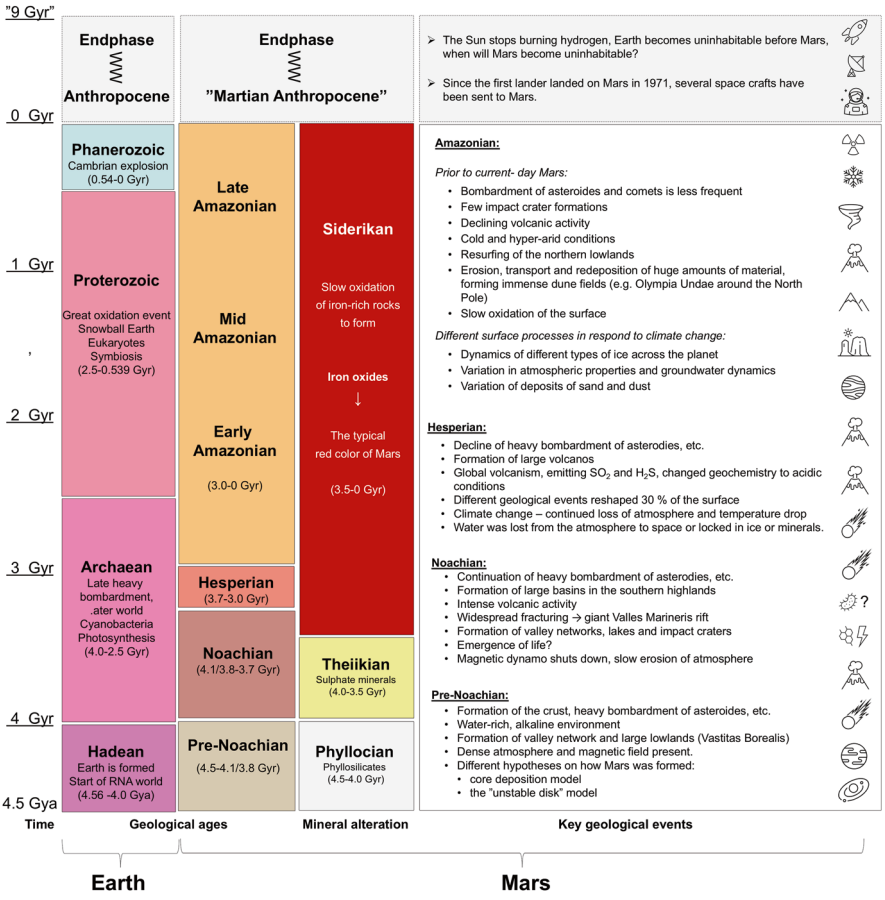

Fig. 2.2 Survey of the geological ages on Mars, based on the classical mineralogical ages based on impact crater rates and predominant type of mineral alteration (Bibring et al., 2006). For comparison, the geological ages for Earth are listed to the left. Original figure by Natuschka Lee

However, early Mars may have been cold and wet, rather than warm and wet. There is also the issue of obliquity cycles. That is, the rapid variation (on geologic time scales) of the planet's rotational axis inclination. This would have had a considerable influence on the shaping of local environments at any time, particularly regarding the possible effects of water on climate and mineralogy. One should bear in mind that over the 400 My span of this water-rich period, Mars would have undergone between 3000 and 4000 such obliquity variations. The same region could have experienced liquid water environments at one moment and 100,000 years later, freezing periglacial conditions. These considerations apply also to the Noachian but perhaps their effect gradually decreased as Mars lost most of its surface water.

The Noachian period (4.1–3.7 Gyr ago) was named after Noachis Terra, a highland region located in the south, between the large Hellas and Argyre impact basins

(Carr & Head, 2010). In this period, the heavy bombardment was intense, shaping the scarred face of the southern highlands and creating the largest impact basins (Argyre, Isidis, and Hellas) one can see today on the surface. Simultaneously, intense volcanic activity took place in many regions of the highlands and in Tharsis. With the built-up of the Tharsis rise, a widespread fracturing took place, and the giant Valles Marineris rift system formed. A warm climate presumably prevailed and precipitations took place. Many dendritic valley networks on the Martian surface date back from this period, as well as lakes in topographic lows and impact craters. A shallow ocean in parts of the northern lowlands may even have existed (Khan et al., 2021). At the end of the Noachian, the planet's interior continued to cool, and the magnetic dynamo shut down (see Sect. 2.2). Furthermore, the slow erosion of Mars's atmosphere began (see further Sect. 2.3).

The Hesperian period (3.7–3.0 Gyr ago) is named after the Hesperia Planum region, a broad lava plain, located northeast of Hellas (Tanaka et al., 2014). During this period, 30% of the Martian surface resurfaced due to a multitude of different geological events. While the impact cratering rate significantly declined with the end of the heavy bombardment, global volcanism continued. Fluid basalts extruded and created the broad highland volcanic features (paterae). In the northern lowlands, enormous volcanic plains developed. Large volcanic edifices developed, such as Tharsis Montes, Arsia Mons, Pavonis Mons, and Ascraeus Mons, which are among the largest volcanoes in the solar system, only surpassed by the younger Olympus Mons which started forming around 3.5 Gyr ago (Fuller & Head, 2002). The extensive degassing of sulphur dioxide and hydrogen sulphide created acidic conditions, which changed the overall geochemistry of Mars. Large sulphate deposits formed, mainly in the wider Meridiani Planum and Vallis Marineris regions. In the Late Hesperian, the atmosphere probably reached its present-day density (Carr & Head, 2010). The formation of valley networks ceased, the temperatures dropped, and most of the water was either lost from the atmosphere to space, trapped in the permafrost or polar caps, or bound in minerals (Carr & Head, 2019). Regional volcanic eruptions, dyke intrusions, and impact events triggered several catastrophic releases from these underground reservoirs and created immense, short-lived flash floods that carved gigantic outflow channels into the surface. The largest of them, for instance, Kasei Valles and Ares Vallis, are found in the Circum-Chryse region and discharged into the Chryse Planitia plains. The Hesperian outflow channels can be spotted in many regions, all over the planet. Collapsed source regions remain with the so-called chaotic terrains, which extend over large areas.

The Amazonian period (3.0 Gyr ago–present) is named after the Amazonis Planitia region of Mars, located in the northern lowlands between the Tharsis and the Elysium volcanic centres (Carr & Head, 2010). This is the longest of the Martian periods. It is characterized by cold and hyper-arid conditions like those observed today. Only occasional and short-lived breakouts to warmer and wetter conditions seem to have occurred, possibly due to impacts, volcanic activity, or changes in the obliquity of Mars (Salese et al., 2016; Wilson et al., 2016). Volcanic eruptions continued with declining eruption rates until very recently (2–5 Myr ago). The Amazonian period is also defined by extensive resurfacing of the northern lowlands.

Wind was a driving factor in remodelling the surface of the broad plains. Erosion, transport, and redeposition of huge amounts of material took place and formed immense dune fields, such as Olympia Undae around the North Pole. Outflow activity still happened in the Chryse region and Amazonis Planitia, but this period has been dominated by glaciation and ice-related surface processes, especially on the flanks of the Tharsis volcanoes, in Hellas and at the dichotomy boundary. As a consequence, the geochemical regime changed towards a slow oxidation of the rocks due to the sparse presence of liquid water (Bibring et al., 2006).

2.2 Mars Geology Today

Current-day Mars is dry and cold (Fig. 2.3). The northern and the southern hemispheres exhibit a sharp contrast, known as the Martian dichotomy, causing an up to 3 km difference in elevation (Watters et al., 2007). The geography and topography of Mars are extreme: the planet harbours the highest mountain, the deepest and longest valley, and some of the largest volcanoes (Olympus Mons, close to three times as high as Mount Everest on Earth) and at least one of the largest canyonlands in the Solar System, making the surface of Mars about three times rougher than Earth's. However, the amount of dry land on Mars is about the same as on Earth (Carr, 2007).

Mars has two permanent large, thick polar ice caps (a large one in the north at Planum Boreum, and a smaller one in the south, at Planum Australe), consisting mainly of water ice and to some extent, depending on the season, of dry ice (solid carbon dioxide) (Foss et al., 2017). The northern plains comprise about one third of the Martian surface and they are flattened by lava flows with few impact craters, while the southern plains (two thirds of the Martian surface, believed to be older than the northern plains) are characterized by highlands and numerous ancient impact craters. A large part of the Martian surface is characterized by igneous rock (tholeiitic) basalt; however, the boundary (the fretted terrain) between the two terrains is generally of unknown composition. The fretted terrain is characterized by a complex mixture of up to 2 km-high cliffs along flat lowlands, lobate debris aprons (rock debris below cliffs), canyons, mesas, buttes, rock-covered glaciers, channels with wide flat floors and steep walls, and deep valleys with lineations with different types of deposits (lineated valley fill, LVF). Mars's surface is dominated by ancient terrains (Noachian and Hesperian) with as much as 50% surface being older than 3.6 Gyr (Neukum & Hiller, 1981).

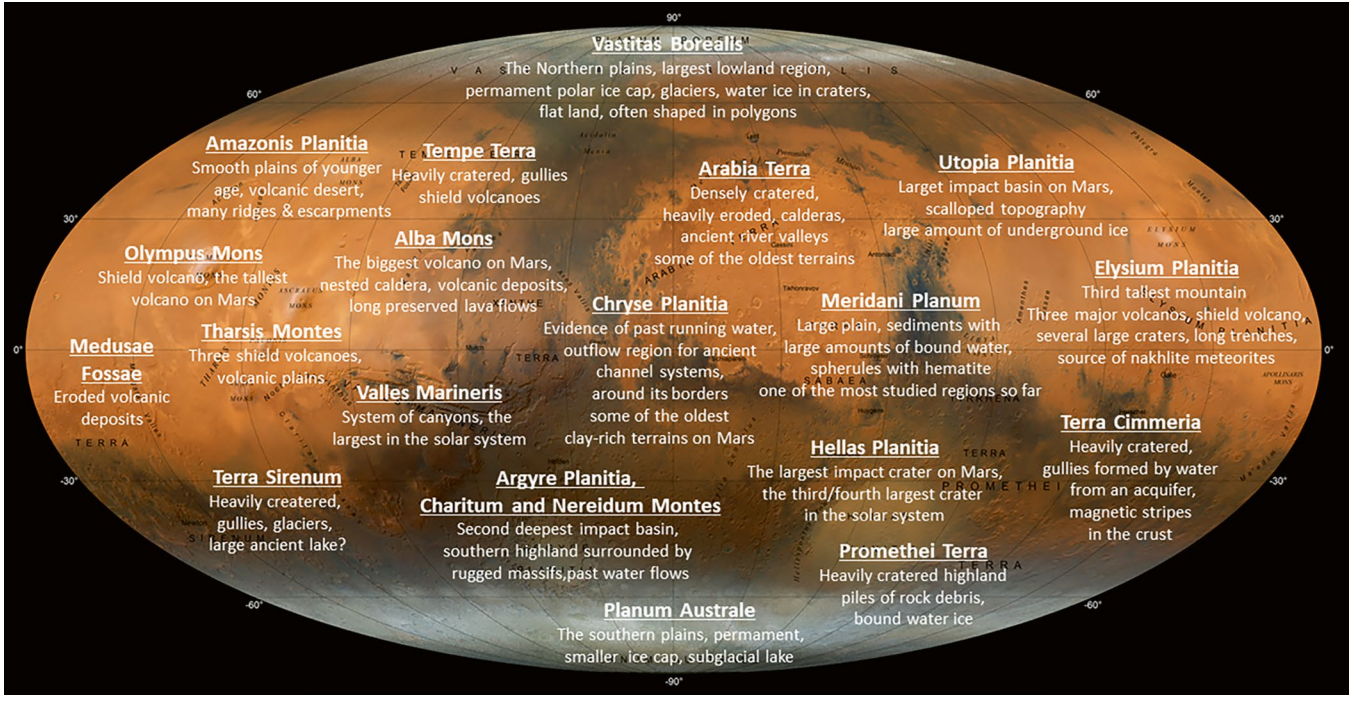

Fig. 2.3 Geological map of Mars today, showing the distribution of a selection of landforms and providing insights into the presence of resources such as frozen water. Original figure composition by Natuschka Lee based on the Mars map background created by the Dr. Dimitra Atri and the New York University Abu Dhabi team (NYUAD), using 2 years of data (>3000 observations) gathered by the Hope probe launched by the United Arab Emirates. Weblink: UAE researchers' Mars map shows Red Planet in striking detail (thenationalnews.com)

2.2.1 Mars Surface and Subsurface Conditions

The surface of Earth is a proxy for its geological history as well as for the evolution of life and the development of multicellular organisms and organized populations such as human civilizations. Today, 95% of the human population, which represents 0.01% of all life on Earth, lives on 10% of the surface of Earth. When considering the settling of humans on Mars, the question is which parts of the Martian surface would be, eventually, suitable for the first attempt. To investigate this concept, we need detailed knowledge on both the surface and the subsurface of the whole of Mars.

2.2.1.1 Current Regolith

Almost all of Mars's surface is covered by a metre-thick, reddish layer of unconsolidated material, typically referred to as regolith (Fig. 2.5) and which often covers the underlying bedrock. The uppermost part of the regolith (10 cm) is referred to as soil and typically consists of grains whose size ranges from dust to pebbles. In contrast to that of the Earth, this soil contains very little organic material. Dust is defined as particles of sizes in the 1–4 μm range.

Larger components of the regolith are derived from local bedrock while smaller components such as soil and dust have regional or even global components. Therefore, the chemistry of larger components will typically be similar to that of the local bedrock while the soil and dust have a very similar chemistry across Mars (Grady et al., 2022) (Fig. 2.4). The most relevant part of the regolith for human exploration is the smaller fraction, including soil and dust, whose size and other characteristics (composition, shape, specific gravity, relative density, cohesion, compressibility, shear strength, and thermal conductivity) make it a hazard for both equipment and humans. The elemental abundance of the soil component is shown in Fig. 2.4 (Grady et al., 2022). It consists of mixed primary igneous minerals (olivine, pyroxene, plagioclase, iron oxides) and altered materials which are partly amorphous (Bish et al., 2013; David et al., 2022; Hausrath et al., 2023). Alteration minerals include clays, iron oxides, and salts such as perchlorates, chlorides, and sulphates (Bish et al., 2013; David et al., 2022; Hausrath et al., 2023; Hecht et al., 2009; Morris et al., 2006; Wang et al., 2020). The Phoenix lander measured ~0.5 wt% of perchlorates and a moderate pH of the regolith of ~7.7 (Hecht et al., 2009). Perchlorates and other salts pose risks to human health and are corrosive to equipment. Experiments performed with Martian soil analogues doped with perchlorates in amounts found in Martian soils showed that this concentration is detrimental to plant growth (Eichler et al., 2021). In addition, nitrates have been detected in Martian dust at concentrations up to hundreds of ppm (Stern et al., 2015). Based on the existence of particle-born life in the atmosphere of Earth (Reche et al., 2018), it has been speculated that the dust could carry microbes (Grady et al., 2022).

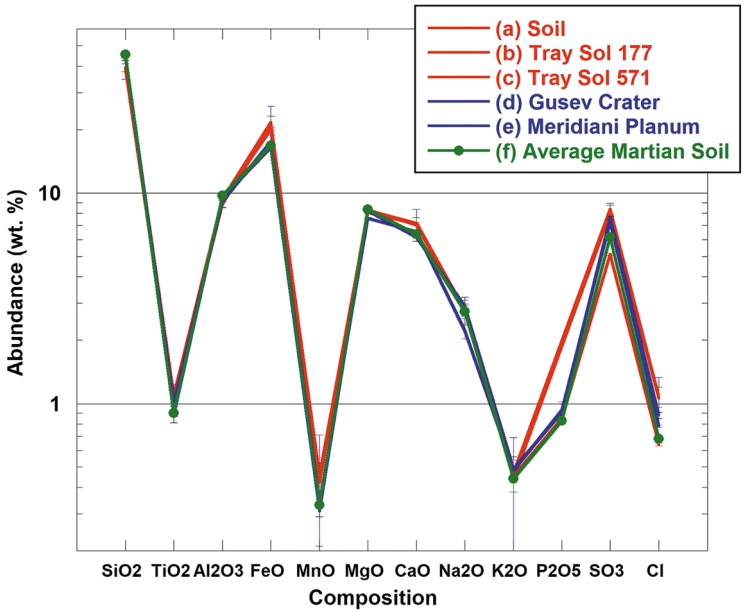

Fig. 2.4 Soil composition across Mars: the diagram shows elemental abundances in form of oxides (reprinted from Grady et al., 2022). Locations (a)-(c) are from Gale Crater

Fig. 2.5 Curiosity's view of Martian regolith and boulders at Dingo Gap (MastCam; February 9, 2014; image transformed to Earth-like atmospheric view). Credit: NASA/JPL-Caltech/MSSS

2.2.1.2 Current Bedrock

The Mars crust has been seen as basaltic since the first Mars missions in the 1960s and 1970s. Orbiters with spectrometers (both near infrared and thermal infrared) have obtained global views of the surface of Mars and showed a predominance of plagioclase and pyroxenes, as expected for basaltic rocks, locally associated with olivine as in the crust of the Nili Fossae region (Bandfield et al., 2000; Mustard et al., 2005). Pyroxenes are present both as low-calcium pyroxene (LCP) such as pigeonite, and high-calcium pyroxenes (HCP) such as augite, but with a distinct proportion between the ancient crust where both pyroxene types are in similar proportion, compared to recent volcanic regions dominated by HCP (Mustard et al., 2005). Gamma-ray spectroscopy was used to map the concentration of several elements such as Si, Cl, K, Fe, and S at a broad scale (>100 km) in the top first metre of the surface (Boynton et al., 2007). This instrument enabled scientists to determine that the crust is significantly richer in Fe (~18 wt% on average) than the mid-ocean ridge basalt on Earth crust (~10 wt%) and contains substantial abundance of sulphur (~6 wt% elemental SO_3). Given the high abundance of iron, the pore-free density of these basalts has been estimated to be ca. 3100–3300 kg/m^3 (Baratoux et al., 2014).

While this first-order view of an iron-rich basaltic planet is still predominant, these results are based on spectroscopic observations (visible infrared, thermal infrared, and gamma-ray spectroscopy) that are only representative of the surface material, leaving unknown a large part of the crust. The last two decades have also provided a lot of new observations that enable us to draw a much more complex picture of the composition of Mars's crust. In particular, felsic rocks including anorthosite and quartz have been detected locally by spectrometers (Carter & Poulet, 2013). Felsic and alkali-rich igneous rocks have been identified on out-of-place blocks and conglomerate clasts analysed by the ChemCam instrument of the Curiosity rover at Gale crater (Mangold et al., 2016; Sautter et al., 2014, 2015; Schmidt et al., 2014). These results have been echoed by the discoveries, in the Moroccan desert, of the Martian meteorite breccia NWA 7034 (paired with NWA 7533 and NWA 7475 of similar origin) that is dated at 4.4 Gyr and contains differentiated rocks with alkali feldspars (Agee et al., 2013; Humayun et al., 2013; Wittmann et al., 2015). The proportion of such more differentiated rocks in the whole Martian crust is still being debated. Phosphate minerals such as apatite (Cl, F), merrillite, and whitlockite have been detected in Martian meteorites (McSween& Treiman, 1998) and on Mars (Corpolongo et al., 2023; Rampe et al., 2017, 2020a, 2020b). Actually, Mars appears quite phosphate-rich, 5–10 times more than Earth (Adcock et al., 2013).

In addition to primary minerals, a huge variety of secondary minerals have been detected by spectrometers and by rovers *in situ*. Hydrous sulphates are present as layered deposits in various regions of the equatorial regions (Gendrin et al., 2005) where the Opportunity rover was able to analyse them in detail (Squyres & Knoll, 2005). Ca- and Mg-sulphates such as gypsum, anhydrite, polyhydrated Mg-sulphates,

and kieserite seem predominant and related to the precipitation of minerals in the presence of water and a sulfur-rich crust (Chipera et al., 2023; Ehlmann & Edwards, 2014; Siljeström et al., 2024; Vaniman et al., 2018). A huge range of clay minerals (phyllosilicates) have been observed in various contexts, including hydrothermal activity, surface weathering, and sedimentary deposits (Carter et al., 2015; Dehouck et al., 2010; Ehlmann et al., 2013; Poulet et al., 2005). While Fe-Mg bearing smectites are predominant spatially, higher-temperature minerals were also observed which include kaolinite, chlorites, talc, serpentine, and prehnite. Hydrogen has been detected by the gamma-ray and neutron spectrometers in the first metre and is bound in minerals and adsorbed water in the near-surface of equatorial regions. In addition, nitrate concentrations up to hundreds of ppm have been detected in mudrocks at Gale Crater (Stern et al., 2015).

Minor elements have been observed by several *in situ* instruments. In Gale crater, copper and zinc have been detected in abundance by the ChemCam instrument, reaching up to 1 wt.% for Cu and 5 wt.% for Zn (Payré et al., 2019). Nevertheless, this is in relation with fracture fills of a few of the outcrops around the location informally named Kimberley, potentially due to localized hydrothermal circulation. Lithium has also been detected by the ChemCam instrument in Gale crater, likely in connection with clay minerals (Frydenvang et al., 2020), but this element is not present in huge abundance (100s of ppm) and could only be observed thanks to the low detection limit of laser ablation spectroscopy. The knowledge of the distribution and abundance of minor elements on Mars is still sparse, limited to the few locations explored by rovers and by their instrument capabilities. Regarding resources available on Mars, Mars displays a diversity of minerals that is close to that of Earth. The mining of useful major elements such as iron or sulphur should be possible, as would the extraction of clays for construction. However, ore deposits on Mars would be limited compared to Earth, because they develop on Earth in relation with plate tectonics, along subduction zones, orogeny, etc., and those ore deposits are the predominant sources of rare earth elements that are of huge importance for the industry, especially for electronic components. On Mars, one can expect impact craters to have created hydrothermal conditions sufficient for ore deposits, but no *in situ* data have shown such deposits and orbital detections within impact craters are still limited to a few common minerals. It is highly uncertain that the minor elements observed locally by rovers could be extracted given their paucity. Lastly, water from hydrated minerals (sulphates and phyllosilicates) is likely to represent the main source of water in the equatorial regions (<25° N and S) where no active glacial landforms have ever been observed.

Most Martian meteorites, which are the only samples of Mars we currently have on Earth, are igneous (no sedimentary ones have been found so far) and almost all of them formed relatively recent (<1 Gyr). The samples (0.5 kg) to be returned from Mars are expected to contain a more diverse mineralogy than Martian meteorites including sedimentary rocks and regolith samples with some dust component (Farley & Stack, 2023; Simon et al., 2023).

2.2.1.3 Organic Content of Bedrock and Regolith

Dust and rocks have been analysed for their organic matter content. When looking today into rocks billions of years old, one of the biggest concerns for the detection of organic matter is the preservation potential of the molecules over geological periods of time, given the harsh radiation conditions and the presence of oxidants such as perchlorates. The ability to detect organic compounds in Martian sedimentary rocks is a function of their initial abundance and entrainment as the rock formed as well as the extent of subsequent degradation during diagenesis, exhumation, and exposure to the surface and near-surface radiation. Their detection then depends on the performance, flexibility, and robustness of operating instruments.

The Sample Analysis at Mars (SAM) instrument onboard the Curiosity rover is an analytical laboratory that has been analysing Martian samples since 2012. Molecules were detected and identified at various locations in Gale crater, by heating up the samples up to 900 °C to release their organic content. The molecules identified were in the form of chlorinated (Freissinet et al., 2015; Szopa et al., 2020) and sulfurized (Eigenbrode et al., 2018) organic compounds up to 300 ppb in weight, long-chain hydrocarbons up to 12 carbons, possibly coming from decarboxylation of long-chain carboxylic acids, and an aromatic acid, benzoic acid. Possible indigenous Martian nitrogen-containing organic molecules have also been detected in sand dunes and rocks of Gale Crater (Millan et al., 2021, 2022). The origins of the molecules detected on Mars so far remain unclear, as they could come either from Martian sources (hydrothermal, igneous, atmospheric, or biological) or exogenous carbon (meteoritic, cometary, or from interplanetary dust particles). More recent findings from the SHERLOC instrument onboard the Mars 2020 Perseverance rover, which currently explores Jezero Crater, include fluorescence and Raman signals that suggest possible one- and two-ring organic molecules (Scheller et al., 2022; Sharma et al., 2023), although inorganic sources such as cerium and defects in silicates can also explain the fluorescence signal (Scheller et al., 2024).

In addition, co-evolving CO and CO_2 in the SAM-EGA (Sample Analysis at Mars-Evolved Gas Analyzer) instrument at the Curiosity rover from samples from the shallow subsurface of Gale Crater at temperatures compatible with oxidation or decarboxylation of organics leads to the conclusion of a higher abundance of organic matter present on Mars (Sutter et al., 2017), up to ppb in weight, possibly ubiquitously on Mars, in the soil and sediments. Certain types of mineralogy favour the long-term preservation of organic matter, such as clays or sulphates. It is no coincidence that the organics-richer sample analysed by Curiosity contained 20% of smectite clay. Samples that have spent most of their time buried and have been only freshly exposed to surface galactic and cosmic rays are also most likely to have preserved organic content.

In situ investigations provide significant progress towards mapping out taphonomic windows of preservation for chemically reduced organic compounds. The ExoMars 2028 Rosalind Franklin rover is designed to enhance the detection, in abundance and diversity, of organic molecules on Mars (Vago et al. 2017). Lessons learned will feed forward to planning of future experiments and increase our ability

to select future landing sites for robotic or crewed mission, in the search for traces of any form of life. In the mid-2030s, samples returned from Mars in the Mars Sample Return (MSR) program would provide the first ground truth of these data, enable the search for other organic molecules that are not detectable by *in situ* instrumentation, and address fundamental questions on the organic material present in Mars's subsurface, as treats or threats for astronauts.

2.2.1.4 Water

The first speculations about the presence of water on Mars were made based on early telescope observations at the end of the eighteenth century, leading to rather spectacular interpretations involving Martian civilizations. As scientific instruments developed, the hypotheses on the presence of water on Mars changed gradually. The first unequivocal detection of water vapour on Mars was not made until 1963. Since then, numerous ground-breaking discoveries have been made around extraterrestrial water. Though Mars appears dry today, if its current known water resources were to melt, they would still cover the surface with an approximately 30 m layer of water (Lasue et al., 2019). Understanding the history and evolution of water on Mars will yield valuable insights into the dynamics of water and how it may influence the geology of different astronomical bodies in the Solar System, as well as how a biosphere could arise or allow Earth-like life to survive.

The history of the water resources on Mars have been perplexingly dynamic, encompassing wet phases, atmospheric exodus, and geologic entrapment of water (Scheller et al., 2021). In the early phase of the Solar System, it has been postulated that the inner planets were too hot to allow water to condense into liquid or ice. Thus, once the inner planets cooled down, new water was delivered to them by asteroids and comets. On Mars, several NASA-ESA missions have shown that water must have been present in large amounts on the Martian surface, up to 100–1000 m global layer of water (GEL), for long periods billions of years ago, and that some of these waters had a significant influence on the Martian surface (Lasue et al., 2019). However, it is believed that Mars has lost large amounts of water throughout its history. The mechanisms behind this loss have not yet been fully resolved, but some plausible hypotheses are that the solar wind stripped away some of the water in the Martian atmosphere and that the remaining parts remained frozen in, for example, the poles. Another possibility is that much of the current water is bound in various minerals such as phyllosilicates, sulphates, opaline silica, and zeolites (Mustard, 2019). It has been proposed that up to 30–99% of Mars's initial water was permanently buried in the crust already by 3 Gyr (Scheller et al., 2021).

Today, surface water ice is only permanently stable in the polar regions. At lower latitudes, it is only found beneath the surface. This is due to the direct relationship between temperature and latitude, which also means that, at locations closer to the equator, ice is buried deeper. The Phoenix lander discovered ice within the top few centimetres of the surface at 68°N (Smith et al., 2009) and fresh impact craters have excavated nearly pure water ice, probably more than 90% by volume, within a metre

of the surface as near to the equator as 43°N (Byrne et al., 2009). Gamma ray and neutron spectroscopy maps revealing water-equivalent hydrogen suggest a widespread ice presence in the mid-to-high latitudes within about 1 m of the surface (Wilson et al., 2018). An ice-rich, latitude-dependent near-surface material varies from a few to tens of metres in thickness in both northern and southern mid-latitudes (Squyres & Carr, 1986). An abundance of glacial features, such as lineated valley fill and concentric crater fill, can be found in numerous regions. Through combined geomorphic and radar analysis, lobate debris aprons have been identified as remnants of nearly pure ice glaciers covered in debris (Holt et al., 2008). Additionally, radar sounding has found subsurface interfaces believed to represent the bottom of massive ice sheets buried in the northern plains region of Arcadia Planitia (Bramson et al., 2015) and Utopia Planitia (Stuurman et al., 2016). Scarps near the latitudes of 55° display thick, massive ice and seem to extend nearly to the surface (Dundas et al., 2018). However, the structure of the near subsurface, including the depth to the ice table as well as the lateral and vertical extent, remains largely unknown, particularly at lower latitudes where the ice is likely less stable.

In summary, the screening of water on Mars remains a crucial task for future Mars missions. Efforts are being made by different institutions to create useful maps of the various water sources there.

2.2.1.5 Mars Subsurface

The thickness of the Martian crust is between 24 and 72 km, depending on the location (Knapmeyer-Endrun et al., 2021). In contrast to the surface, the subterranean sphere offers shelter from extreme weather and temperature variations, radiation, and meteoroid and asteroid falls. Exploring the subterranean sphere on Earth as well as on other planetary bodies like Mars helps us understand both the complex construction and the history of a planet, and geological phenomena such as earthquakes and volcanoes. On Earth, the subsurface has also been an important source for many valuable natural resources, such as groundwater, minerals, metals, and energy (oil, gas). The same, for certain aspects, is expected to be true for Mars. Figures 2.6 and 2.7 show the modelled underground temperature and depth of ground water on Mars.

Mars also harbours large amounts of caves. Caves (or caverns) are usually described as natural cavities in a rocky environment where at least some part is dark, be it in the subsurface or inside mountains or lava from volcanic vents. Since the early beginning of human history on Earth, caves have played an important role in different ways, from dwelling sites for early humans to fascinating exploration sites for interdisciplinary science fields, such as geochemistry, hydrochemistry, geomicrobiology, and geo-biotechnology. Cave-based sciences play an important role in exploring the history of Earth, in the survey of valuable resources such as aquifers, and for expanding our concepts about the boundaries of life and the evolution of dark life ecosystems (Lee et al., 2012). A recent study concluded that caves, or at least subsurface access points (SAPs) are expected to be ubiquitous across the whole solar system, from Venus to Pluto, on rocky or icy bodies (including comets)

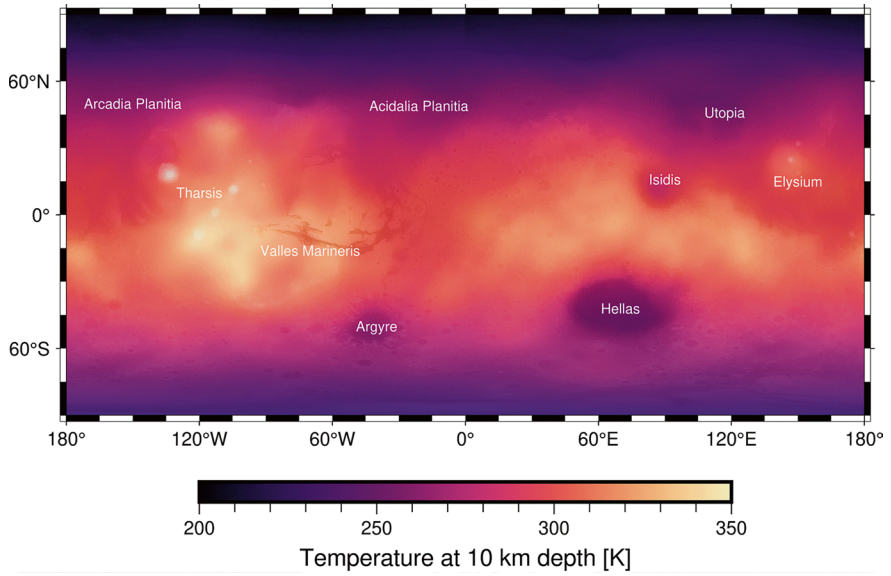

Fig. 2.6 Cartesian map showing modelled temperature at 10 km depth on Mars. Courtesy of Ana-Catalina Plesa

of a size sufficient to allow at least one of the six speleogenic processes recognized

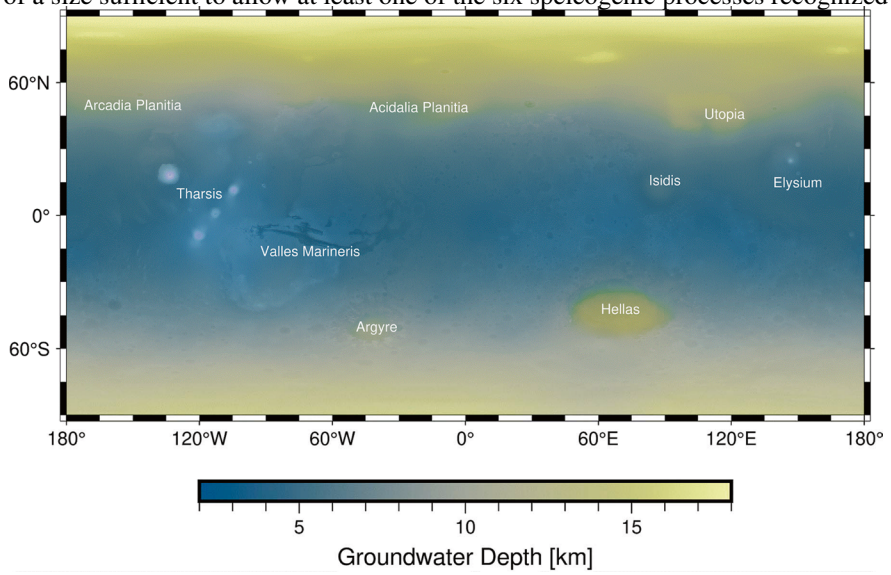

Fig. 2.7 Cartesian map showing modelled depth beneath the surface of Mars where groundwater is expected to be found. Courtesy of Ana-Catalina Plesa

so far for cave formation (Wynne et al., 2022a, 2022b). To date, the bulk of our knowledge is based on high-resolution imagery data on SAPs on Mars (>1162 SAPs) and on the Moon (>276 SAPs). The majority of the SAPs on Mars are found in volcanic edifices and lava fields, with several different morphologies. The width of these cave entrances is around 100–250 m, and their depth is believed to reach at least 130 m. Approximately seven SAPs are believed to be found in a karst-like terrain and may thus contain dissolution caves, which may have been formed by draining surface water or by acting as pathways for hypogenic fluxes (Parenti et al., 2020). Theoretically, caves could be useful for the first settlers of Mars, since they can provide protection from intense solar radiation, micrometeorites, dust storms, and extreme temperature fluctuations. Further, they may also serve as an access route to explore potential resources for industrial activities as well as the geological, palaeohydrological, and potential biological histories of Mars. However, so far, none of the SAPs have been verified as 'genuine' caves—thus, physical evaluation on site is needed before further realistic plans can be made about the usefulness of SAPs on Mars for future settling.

2.2.2 Mars Interior

The shaping of a planet and its surface is complex, based on a multitude of different processes in the core of the planet, such as the generation of the magnetic field and heat, which in turn influence processes such as volcanism and tectonics.

Beyond the regolith layer lies the bedrock, which consists of solid rock. The internal structure of Mars is differentiated like that of the Earth, and the inner part consists of a metallic core overlaid by less dense materials. During the last years, several new observations revealed the nature of the Martian bedrock and core, confirmed the size of the molten core (radius 1830 km), and described some of the characteristics of the Martian mantle and its different crusts (Khan et al., 2023; Stähler et al., 2021). For a long time, it was believed that Mars was tectonically inactive, but like the surface of the Earth, the surface of Mars has evolved significantly throughout time, however in quite different manners. In contrast to the Earth, Mars does not have several continental plates but one big continental plate. Still, it is believed that the surface of Mars was also shaped by various tectonic processes. Even today, rock fractures can form in the Martian crust, and since November 2018, the InSight mission has recorded more than 1300 seismic events on Mars (Banerdt et al., 2020). Monitoring marsquakes has revealed several interesting new features, such as that the thickness of the crust of Mars is about 70% thicker than the crust of the Earth, and that it is inconsistent across Mars, thus possibly explaining the significant elevation difference between the northern and the southern parts. Thanks to these observations, it also became possible to hypothesize that a large fraction of heat producing elements are confined in the crust rather than in the underlying mantle, which in a longer term could imply that Mars still has some volcanic activity (Fernando et al., 2023; Giardini et al., 2020; Kim et al., 2023).

2.2.2.1 Internal Evolution and Volcanism

Mars is smaller than the Earth: its mean radius is 3390 km while the mean radius of the Earth is 6371 km. One could therefore expect that Mars has cooled down more rapidly than the Earth, since heating is by a large factor driven by radiogenic heat sources distributed in the mantle, whose volume scales with planet radius cubed, whereas cooling occurs at the planetary surface, which scales with radius squared. A smaller planet should therefore cool much faster than a larger planet. However, there is a fundamental difference between the two planets: Mars is a one-plate planet (also called a stagnant-lid planet) while the Earth has plate tectonics. On Earth, this leads to efficient cooling of the mantle by subduction of cold plates into the mantle, and increased heat loss at the surface at diverging plate boundaries.

Telluric planets have formed by accretion from the solar system disk of dust and gas. During their formation stage, high-density materials sink towards the centre, resulting in a planet differentiated in a metal core and a silicate mantle. The evolution of the upper part of the mantle, the lithosphere, and (at least in the case of the Earth) the onset of plate tectonics is affected by several factors, among which the most important ones are the planet size, the temperature, and rheology (e.g. Stamenkovic & Breuer, 2014). During the formation stage of terrestrial planets, it is expected that large fractions of the mantle are molten (possibly multiple times) due to large impacts, leading to a magma ocean. The processes of magma ocean formation and solidification are important for the later onset of thermally driven mantle convection and plate tectonics (see, e.g., Elkins-Tanton, 2012). At the beginning of its evolution, Mars formed its core, and this event was accompanied by a large-scale silicate differentiation of the Martian mantle and by crust formation. Using isotopic analysis on Martian meteorites, Kruijer et al. (2020) showed that this event likely happened during the first tens of million years (Myr) of the Solar System's evolution. The solidification of a global magma ocean may have led to a heterogeneous mantle, which may never have efficiently mixed (Plesa et al., 2014). This is supported by Barnes et al. (2020), who demonstrated by using light and heavy hydrogen D/H (deuterium/hydrogen) isotopes, that the Martian crust has had a constant D/H ratio over the last 4 billion years and that there were two isotopically distinct reservoirs in the Martian mantle. The presence of two mantle reservoirs indicates that the mantle is heterogeneous and has not mixed. The present-day thermal state of Mars and its evolution can be constrained from geophysical data, assumptions about its bulk composition and formation history. While studies that analyse the long-term tidal interactions between Phobos and Mars and the orbital evolution of Phobos around Mars provide constraints about the thermal history (e.g. Samuel et al., 2019), the present-day thermal state can be inferred from the actual measured secular acceleration of Phobos orbiting Mars (e.g. Nimmo & Faul, 2013) or from the very recent seismic and geodetic observations obtained during the NASA InSight (Banerdt et al., 2020) mission (Khan et al., 2021; Le Maistre et al., 2023; Stähler et al., 2021; Samuel et al., 2023; Khan et al., 2023). Studies that inform about the present-day thermal state based on geophysical data usually assume that

the mantle is chemically homogeneous, although it has been reported recently (Samuel et al., 2022) that a chemically isolated reservoir located at the bottom of the mantle can be in agreement with InSight data (Le Maistre et al., 2023; Samuel et al., 2023; Khan et al., 2023). Geodynamic modelling has been utilized to infer Mars's present-day thermal profile, mantle viscosity, and heat producing radiogenic elements, incorporating constraints derived from seismological data, geodesy observations, and crust thickness determinations (e.g. Plesa et al., 2022). The present-day surface heat flux of Mars is found to vary between 15 and 33 mW/m^2 and the core-mantle boundary (CMB) temperature is estimated to be close to 2000 K. However, if a molten chemically isolated reservoir exists at the bottom of the mantle the CMB temperature can be significantly larger (Samuel et al., 2023).

Further information on the thermal state is gained if the recently obtained geophysical constraints are included in global geodynamic models of Mars. Plesa et al., (2022) demonstrated that the magnitude of surface heat flow and elastic thickness variations depends on the magnitude of crustal thickness variations. These authors discuss several possible crustal models based either on a two-layer crust with strong seismic discontinuities (at depths of about 8 and 20 km), or on a three-layer crust that included a third layer (with a weak discontinuity at about 39 km depth). Plesa et al. (2022) also show that mantle plumes and cold downwellings may be present in the interior of Mars at present day and would lead to temperature variations in the interior and to variations in the thermal lithosphere thickness. The convection patterns in the mantle are characterized by the presence of several mantle plumes and downwellings, with stronger plumes preferentially focused in the Tharsis region due to the existence of a thick insulating crust at this location, which is directly linked to the volcanic history of that region.

Mars has important volcanoes, which are highly visible on images of the Martian surface. They are in the province of Tharsis. The largest volcano of the Solar System is on Mars; it is Olympus Mons (600 km wide and 27 km high). Three other volcanoes, Ascraeus, Pavonis, and Arsia Mons, are also situated in the Tharsis province. They were all initiated in the Noachian, more than 3.8 Gyr ago. There are low-shield volcanoes as well, such as the Elysium volcanic province or the Syrtis Major volcanic province. Besides the most dominant volcanic Tharsis region and the low-shield volcanoes, there are small early Noachian volcanoes (with diameters ranging from 50 to 100 km and heights of 2–3 km) in the circum-Hellas-basin volcanic province. The volcanoes in both regions were mainly formed in the Noachian to early Hesperian periods (3.7–3.6 Gyr). But volcanic activity persisted after that period until recently: lava flows as young as 2 Myr have been discovered (Hauber et al., 2011; Neukum et al., 2004). Horvath et al. (2021) or Broquet and Andrews-Hanna (2022) have also identified an active mantle plume in the Elysium Planitia region (south of Elysium volcanoes) and hypothesize the presence of an active mantle plume underlying the region.

2.2.2.2 Magnetic Field

Among the four rocky planets in the solar system, Earth is today the only one with a strong magnetic field. This field is pivotal to Earth's biosphere for several reasons, the most important being that it produces a protective shield against, e.g., cosmic radiation, such that Earth's atmosphere and water are not stripped out to space.

Although the liquid core state of Mars was inferred from measuring tides, monitoring its rotation, and acquiring seismic data (Yoder et al., 2003; Stähler et al., 2021; Le Maistre et al., 2023), Mars at present does not possess a global magnetic field. However, early in its history, 4 billion years ago, it harboured a dynamo in its core (e.g. Mittelholz et al., 2020). The presence of an early dynamo was deduced from remnant magnetization in the southern hemisphere, which was observed by the Mars Global surveyor spacecraft and more recently by MAVEN. No crustal field was observed in the Martian northern lowlands. In the heavily cratered and old surface of the south, alternating stripes of positive and negative remnant amplitudes were observed (Acuña et al., 1999). The lineation of the stripes (long E–W trending alternating stripes, see Figure 1 of Connerney et al. (1999) is of course damped out when looking from the point of view of the spherical surface. These stripes, however, are not linked to a plate-tectonics-like behaviour as on Earth, but are either attributed to repeated dike intrusions (Nimmo, 2000) or to a non-dipolar magnetic field (Dietrich & Wicht, 2013). The dichotomy in the remnant magnetic field observation could come from a demagnetization related to rock melting after a giant impact (Connerney J.E.P. et al., 2005). Another explanation has been provided by Zhong and Zuber (2001) (see also, e.g., Roberts & Zhong, 2006), where degree-1 mantle convection with one upwelling in one hemisphere and one downwelling in the other hemisphere can produce a single-hemisphere dynamo. However, magnetized crust in the low-land northern hemisphere may also be covered by dust and may be as old as the southern hemisphere (Frey H.V., 2006) and therefore older than the end of the magnetic field, which is assumed to have ended before the Hellas impact basin 3.9–4.1 Gyr ago (Acuña et al., 1999; Hood et al., 2003; Lillis et al., 2008a, 2008b).

2.2.2.3 Gravitational Field

The gravitational field of Mars is the consequence of its internal and surface mass distribution. It has been measured with high accuracy from orbiting spacecraft (e.g. Genova et al., 2016; Konopliv et al., 2016, 2020; Marty et al., 2009; Smith, 2009). The gravitational field is expressed using spherical harmonics that can represent global (low-degree) features as well as small-scale (high-degree) anomalies. One individual spacecraft is not sensitive to all intermediate degrees and orders as these depend on the orbit geometry as well as the geometry of the measurements from the Earth ground stations (orbit edge-on or face-on). For this reason, researchers working on the determination of the gravity field combine different spacecraft. The last static gravity field determined around Mars was provided by Konopliv et al. (2016).

It must be noted that the gravity field may be described by a geoid, which represents the shape of an equipotential surface. The geoid height with respect to the mean radius can vary within the range of −12 to +8 km. When compared to the hydrostatic figure of the planet, the geoid depicts values between −1 and +2 km (Wieczorek et al., 2019). There are also time variations of the field related to changes in the masses in the atmosphere. They can be used to constrain the dynamics of the Martian atmosphere and icecaps. The static field is used together with the topography to determine the thickness of the Martian crust (e.g. Wieczorek et al., 2022; Wieczorek and Zuber 2004). The admittance obtained from this data allows to characterize the compensation of surface features and the thermal evolution of the planet.

2.3 Mars Atmosphere and Climate

The atmosphere and the climate are two important features which define the environment of a planetary body and determine its potential for habitability. Therefore, a better understanding of the atmosphere and climate on Mars is important to predict how humans and hardware can cope during long stays on Mars.

2.3.1 Atmosphere Composition

The main components of the Martian atmosphere are (values are typical annual means) 96% carbon dioxide (CO_2, can vary by up to 25% seasonally), 1.9% dinitrogen (N_2), and 1.9% argon (Ar) (see Fig. 2.8) (Rafkin et al., 2013). A minor fraction of the atmosphere consists of the so-called trace gases, which including 0.13 wt% dioxygen (O_2), 0.07 wt% carbon monoxide (CO), 0.013 wt% nitrogen oxide (NO), 2.5 ppm water (H_2O), neon (Ne), Krypton (Kr), and Xenon (Xe) (Rafkin et al., 2013). Small amounts of methane have been detected by Curiosity and various orbiters and Earth-based telescopes, which is surprising considering the short half-life of methane in the Martian atmosphere (Formisano et al., 2004; Mumma et al., 2009; Webster et al., 2015). The TGO (Trace Gas Orbiter) failed to detect any, indicating that methane could only be present at very local scale (Korablev et al., 2019).

Atmospheric water is detectable near the surface very close to the exposed regolith between ~0% and 100% relative humidity, which is changing in diurnal cycles. Changes in the amount of dust in the atmosphere, which can be large due to diurnal or seasonal wind events—up to global planetary dust storms—should not be neglected.

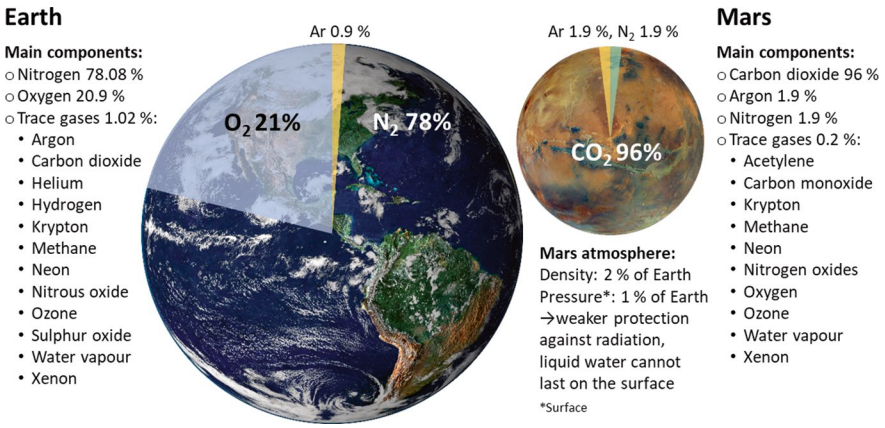

Fig. 2.8 Comparison of the atmospheres of Earth and Mars. The listed values are approximate averages, since some of the values may vary with season. Original figure composition by Natuschka Lee, based on publicly available photos of Earth and Mars. Image credit of Mars: ESA/DLR/FU Berlin/G. Michael. Image credit of Earth: https://eoimages.gsfc.nasa.gov/images/imagerecords/0/885/modis_wonderglobe_lrg.jpg

2.3.2 Current Climate of Mars

Most life forms on Earth seem to have evolved circadian rhythms that allow them to anticipate, prepare, and exploit dynamic resources, such as light, food (prey, growth of plants, etc.), and weather. To mark the time on Mars, it is common to use the local time in Martian hours, which corresponds to a sol (a day on Mars) divided by 24, and the areocentric longitude of the Sun (Ls) as viewed from the centre of Mars. This is equivalent to ecliptic longitude (Ls). The Martian year starts and ends with the northern spring equinox, which is defined as the Martian solar longitude Ls 0. The solar day on Earth (24 h and 11 min) is fairly similar to that on Mars (24 h 37 min). However, the year is about twice as long as on Earth (Fig. 2.9).

The atmosphere of present-day Mars has a very low density, and its average pressure at ground level is about 6 mbar, which is only about 1% of Earth's atmospheric pressure at sea level. The pressure varies depending on the altitude and the season. The seasonal changes in atmospheric pressure are due to the fact that CO_2, the main constituent of the Martian atmosphere, condenses and freezes to CO_2 ice at polar regions during the winter and therefore decreases the atmospheric pressure (Rafkin et al., 2013). The opposite happens in summer when CO_2 ice sublimates and returns CO_2 to the atmosphere and therefore increases the pressure. As there are two polar caps, the pressure is highest around the summer and winter solstices. Figure 2.10 shows the variation between two Viking lander sites during 1 Martian year with the highest pressure recorded during the northern winter solstice (summer solstice at the Martian southern hemisphere) and the lowest at the northern autumn equinox. The measured pressure is different for the two Viking Landers due to Viking 2 being about 900 m lower than Viking 1.

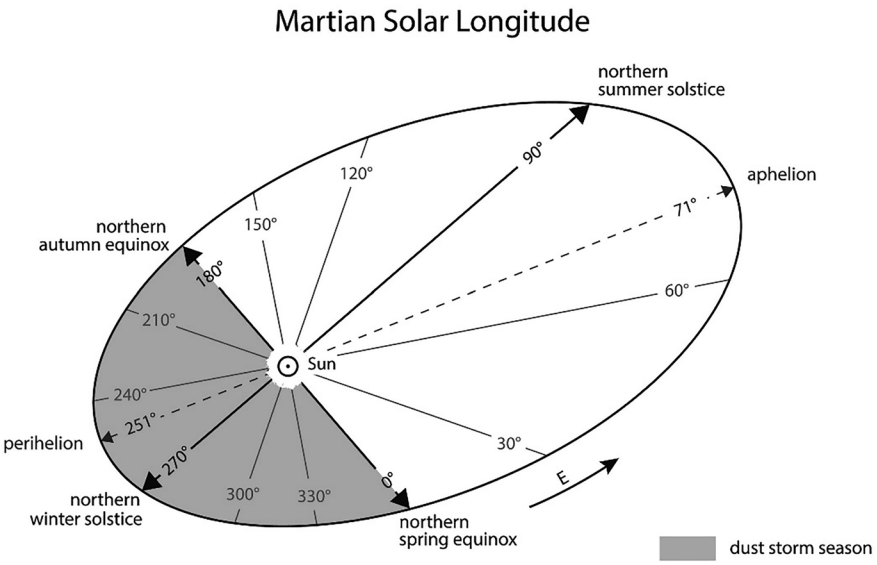

Fig. 2.9 Martian solar longitude. A Martian year is 668.59 Martian days (sols) long, which is equal to 687 Earth days, because a sol is 24.623 h long, ~40 min longer than a day on Earth (Clancy et al., 2000). Reprinted from Pál et al. (2019)

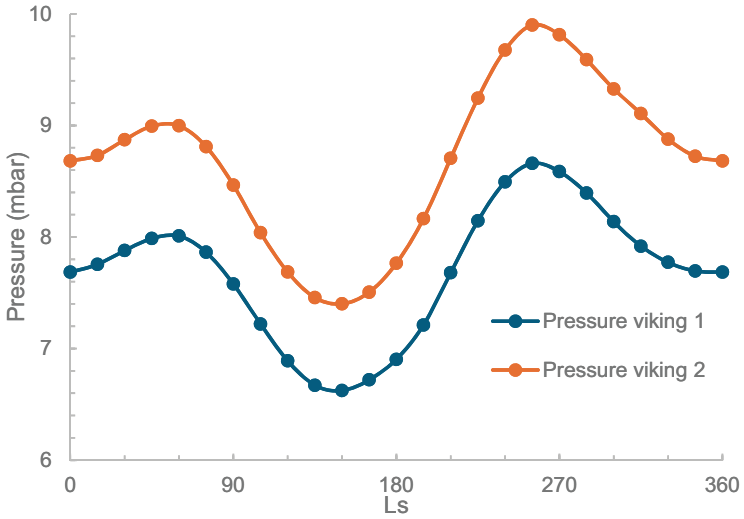

Fig. 2.10 Atmospheric pressure data from the two Viking landers during 1 Martian year. Atmospheric pressure at the surface of Mars varies over the course of the year with the ebb and flow of the seasonal polar caps. (Reproduced from Viking data using Mars Climate Database (MCD-v6.1), 2024)

The temperature range on Mars also varies with day-night cycles, time of year, and latitude. The planetary mean value is about −55 °C to −60 °C at the surface. The highest temperatures, up to about +27 °C, are observed at the equatorial regions and the lowest, down to −143 °C, are reached in the polar regions (Dickson et al., 2013). Figure 2.11 shows variations in temperature at the surface during a sol in different seasons, at the equator, while Fig. 2.12 shows nighttime temperature variations across the surface of Mars.

The relative humidity on the surface of Mars varies according to the time of the day, season, altitude, latitude, and longitude, from below detection limit (0%) to 100% (Figs. 2.13 and 2.14). The driest time is about midday and the highest relative humidity values are detectable in the night up to the early morning. During the most humid conditions, between midnight and 6 AM, brines might form on a few sols—as happened at the Phoenix landing site, close to the north pole—via deliquescence (Fischer et al., 2019), i.e. the formation of a solution on the surface by absorption of moisture from the atmosphere.

The climate on Mars is affected by the abundant dust, which absorbs and scatters visible and solar light and therefore affects atmospheric temperatures and hence winds (Haberle et al., 2017; Rafkin et al., 2013). For example, the dust cover increases the albedo which lowers the daytime warmup. The abundant dust also produces frequent dust devils and dust storms. Dust devils are particle-loaded vertical convective vortices characterized by high rotating wind speeds (estimated to reach up to 100 m/s), significant electrical fields, and low pressure (Balme & Greeley, 2006). The dust devils on Mars are frequently up to a few kilometres high, hundreds of metres in diameter (with narrower bases and broader tops). Most occur

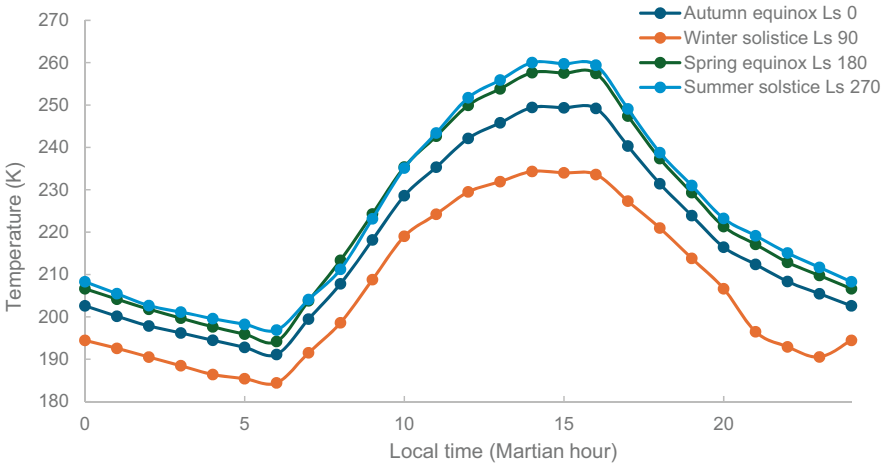

Fig. 2.11 Daily temperature variations in different seasons. Reproduced using Mars Climate Database (MCD-6.1, 2024) with climatology average solar scenario, latitude 0° N, longitude 0° E, and altitude 1.5 m. Note that 180–270 K equals to −93 °C to –3 °C

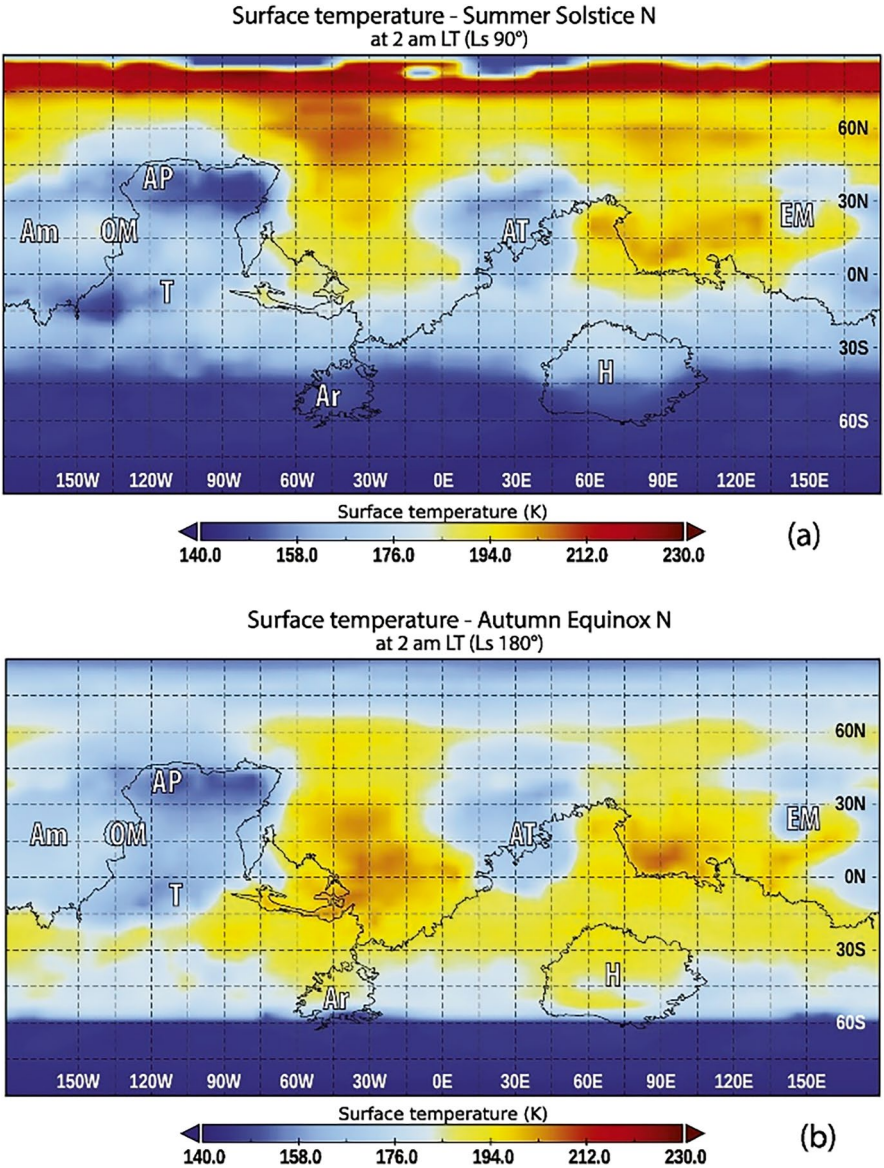

Fig. 2.12 Seasonal dependence of the nighttime surface temperatures. Data from GCM (Global Climate Model) at the northern summer solstice (**a**) and northern autumn equinox (**b**), at 2 AM LT everywhere. Amazonis (Am), Olympus Mons (M), Tharsis Montes (T), Olympus Mons (OM), Alba Patera (AP), Arabia Terra (AT), Elysium Mons (EM), Hellas Plantia (H) and Argyre Plantia (Ar). Reprinted from Pál et al. (2019). Note that 140 K–239 K equals to −133 °C to −34 °C

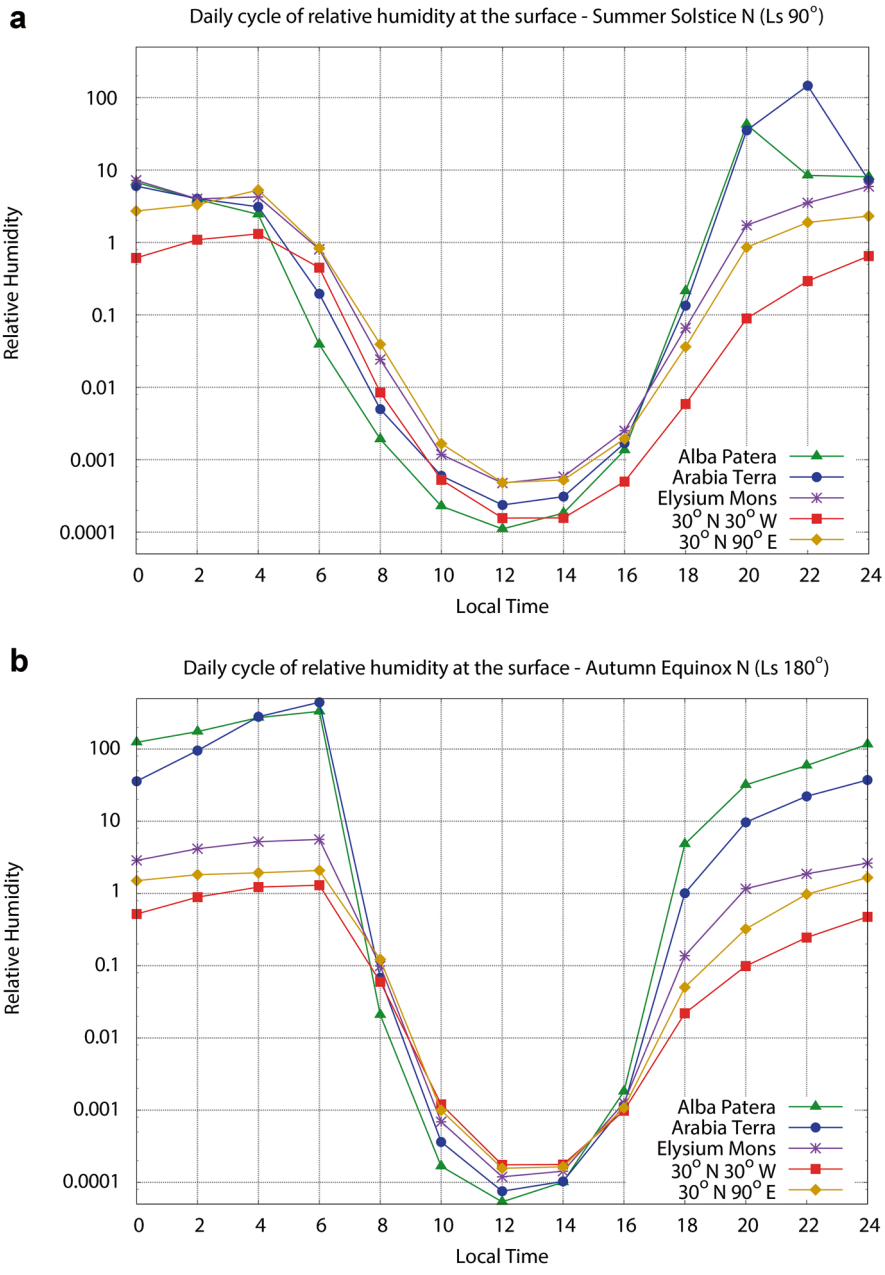

Fig. 2.13 Daily cycles of near-surface humidity at the northern summer solstice and northern autumn equinox (northern summer solstice—Ls 90; Fig. 2.13a) and (northern autumn equinox—Ls 180; Fig. 2.13b) calculated from GCM (General Circulation Model) data. The five locations examined are Alba Patera (30° N 120° W), Arabia Terra (30° N 30° E), Elysium Mons (30° N 150° E), one location at 30° N 30° W and the other at 30° N 90° E. Modified from Pál et al. (2019)

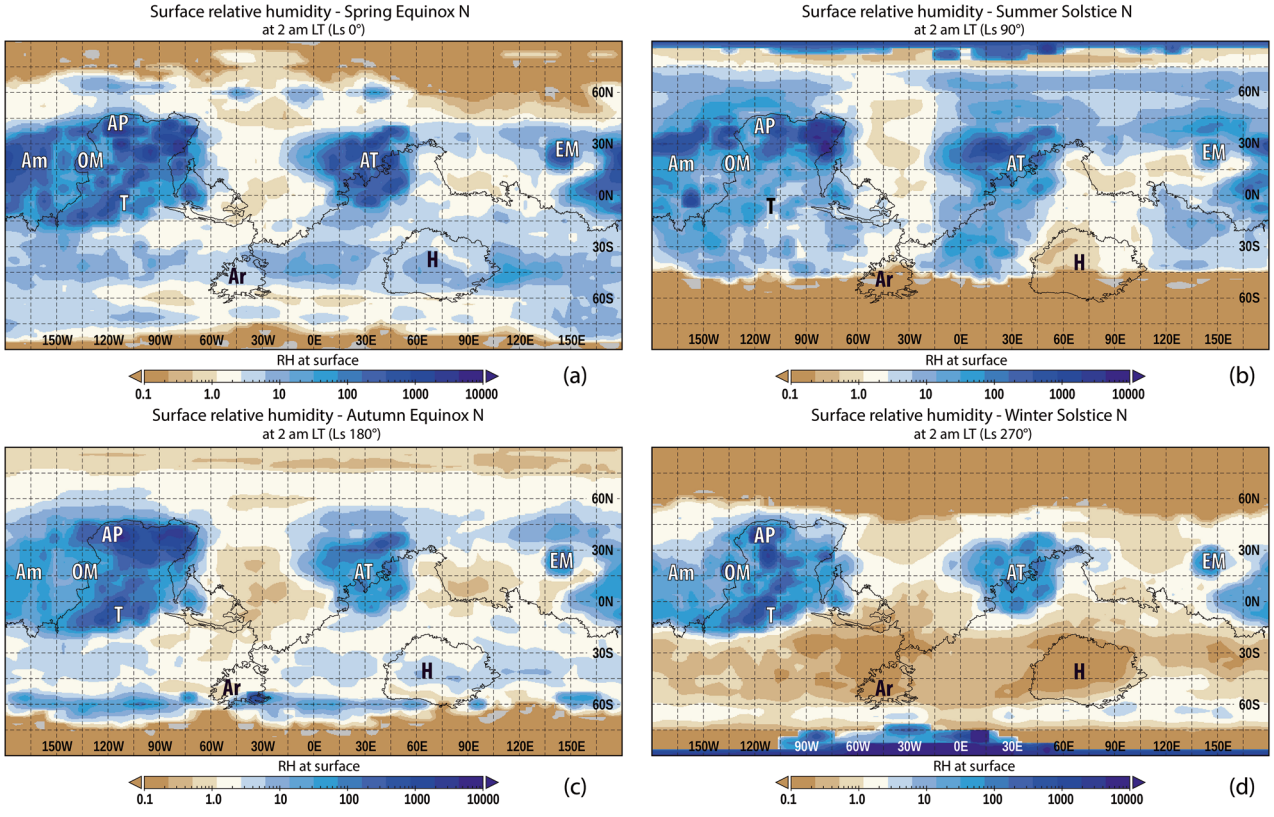

Fig. 2.14 Seasonal dependence of the nighttime humidity distribution. The relative humidity values were derived directly above the surface from GCM model calculation at the time of northern spring equinox (**a**), northern summer solstice (**b**), northern autumn equinox (**c**), and northern winter solstice (**d**), 2 AM LT at everywhere on the map. Amazonis (Am), Olympus Mons (M), Tharsis Montes (T), Olympus Mons (OM), Alba Patera (AP), Arabia Terra (AT), Elysium Mons (EM), Hellas Plantia (H) and Argyre Plantia (Ar). Modified from Pál et al. (2019)

during spring and summer (Balme & Greeley, 2006). It is believed that dust devils are part of the reason for the haze of dust observed on Mars.

Another prominent feature of Mars is dust storms, with speeds up to 160 km/h. They are large (some of the largest in the solar system) and can cover the whole planet, block out the sun and last for weeks or even months (Wang & Richardson, 2015). They preferentially occur in places and seasons—typically, northern autumn and winter (Ls 135–360°; dust storm season)—with above-average surface wind stress (Guzewich et al., 2017; Rafkin et al., 2013; Wang & Richardson, 2015). Global dust storms tend to appear roughly every 3 years (Rafkin et al., 2013). Figure 2.15 shows the distribution of dust during such as dust storm event during Mars Year 34 (1997–1998).

2.3.3 *Fields, Currents, and Escapes*

Today, Mars has a tenuous atmosphere and no global magnetic field and consequently the surface is almost not protected from hazardous external radiation. A magnetosphere, as exists for Earth, forms where flowing plasma (solar wind) is deflected around a planetary object by magnetic fields. In the absence of a magnetic field, solar wind induces a stronger escape of the atmosphere. However, the relevance of a magnetic field for the shielding of an atmosphere has been strongly

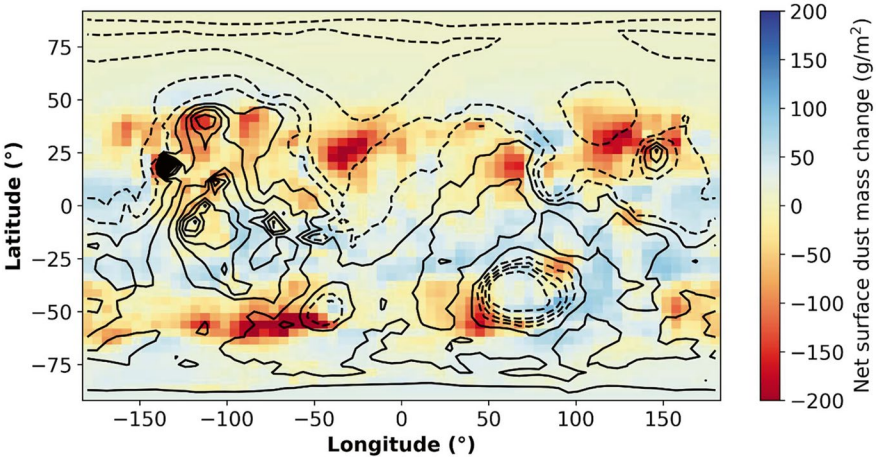

Fig. 2.15 Net surface dust deflation and accumulation throughout the Mars Year 34 global dust storm (Ls 180° to 300°), as simulated by the LMD Mars Global Climate model. A change by 100 g/m² corresponds to a dust layer thickness change of approximately 100 µm. The model assimilates interpolated maps of the column dust optical depth from remote sensing observations (Montabone et al., 2020). The black lines show the Martian topography. Credit: Demetrius Ramette

debated, since observed mass escape rates from Earth, Venus, and Mars are relatively similar, even though only Earth has a magnetosphere (Way et al., 2023).

Escape proceeds through several mechanisms: the removal of neutral particles (thermal escape, photochemical escape, and sputtering) and the removal of ions (ion pickup, magnetic shear and tension-related escape, and pressure gradients). Gunell et al. (2018) have modelled the effects of a global magnetic field on these major atmospheric escape processes and have shown that the escape rate can even be higher for a magnetized planet over a wide range of magnetizations, due to the escape of ions through the polar caps and cusps. It must be noted that this modelling of escape rates depends on the solar flux in all frequencies (X-ray, UV, and extreme UV radiation), on the properties of the solar wind and the atmosphere, which all change over the lifetime of the planet (Lammer, 2013).

Although Mars lacks an Earth-like global magnetic field, it has an ionosphere that results from its upper atmosphere being ionized by solar radiation. This ionosphere is also a highly conductive obstacle to the solar wind plasma.

Related to the magnetic field, there is the potential of having plasma and induced electric currents around Mars, which would help shield the surface from ionizing radiation. Indeed, there is an induced magnetosphere around Mars as Mars is conductive and there are electrodynamic interactions with a magnetized flowing plasma, such as the solar wind. This implies the existence of induced currents (Ramstad et al., 2020). Five years of magnetic field measurements from the Mars Atmosphere and Volatile EvolutioN (MAVEN) orbiter have been used by these authors to map these currents. They found an asymmetry between the northern and southern hemispheres, probably due to the difference in current closure that occurs in the polar regions and found a twist in the near-Mars current system (Sunward current) due to the presence of electric connection between the ionosphere and the solar wind.

2.4 Mars in Its Cosmic Environment

Mars is embedded in the solar system and will therefore be affected by its environment in a multitude of ways—which in turn will influence its potential for habitability for life as we know it. One significant influence is of course the radiation that is emitted from the Sun and from other astronomical bodies outside our solar system. Another significant influence is that of the debris falling to the surface of Mars from space.

2.4.1 Frequency of Meteorite and Asteroid Bombardments

Mars has been subject to bombardments since its formation, as recorded on its surface. So far, hundreds of thousands of impact craters larger than 1 km have been found there, with over 40,000 larger than 5 km wide. Most of these impacts

took place in the Noachian (Scott & Carr, 1978; Tanaka, 1986), but impacts are still occurring (Garcia et al., 2022). Current-day impactors can be divided into several categories: comets, with nuclei ranging between 0.34 and 56 km (Meech et al., 2004); asteroids, ranging from 1 m (Rubin & Grossman, 2010) to 1000 km; meteoroids, 30 μm to 1 m; and micrometeoroids and interplanetary dust particles in general smaller than meteoroids (Rubin & Grossman, 2010). Of these categories, dust and micrometeorites have the largest contribution to the current-day impacts, with a global estimate between 0.71 and 2.96×10^6 kg/year (Nesvorný et al., 2011; Borin et al., 2017; Crismani et al., 2017). Geocentric velocities of micrometeorites have been estimated from observations to be between 15 and 50 km/s (Janches et al., 2003), and micrometeorite craters between 1 μm and several mm have been observed in lunar rocks (Hörz et al., 1971) and space station materials (e.g. Smirnov et al., 2000). Micrometeorite impact velocities for Mars recently have been estimated between 5.7 and 15 km/s (Tomkins et al., 2019), potentially leading to impact craters of similar dimensions as in lunar rocks and space station materials. Considering the damage done on space stations, micrometeorites are an impact phenomenon to be considered in habitat and equipment design. Impact velocities for comets and asteroids on Mars are generally estimated at around 35 km/s for comets and between 7 and 10 km/s for asteroids (Ivanov, 2001; Head et al., 2002; Artemieva & Ivanov, 2004; Frantseva et al., 2018). In addition to crater formation—with crater size depending on impact velocity, impactor material, and impacted material (Holsapple, 1993; Holsapple & Housen, 2007)—a 7.1 km/s impact of a 1-km asteroid can result in a layer of ejecta hundreds of metres thick within tens of metres of the impact crater, tapering off to centimetres at a distance of 500 m (Frantseva et al., 2018). Impact estimates of asteroids and comets have been calculated based on the asteroid and comet distributions tabulated in the Minor Planet Center Orbit Database (MPCORB). These calculations yielded impact rates of 4.34×10^{-3} comets/Myr and 3.3 asteroids/Myr, which are much lower than the annual influx of micrometeorites and interplanetary dust and also lower than the current estimate of an asteroid impact on Earth in the next 900–1000 years (Fuentes-Muñoz et al., 2023).

2.4.2 Radiative Environment

When preparing for human missions, Mars's current radiation environment needs to be considered. This is particularly true of ultraviolet (UV) and ionizing radiation, because of the danger they pose to humans (see Sect. 6.4.3). By definition, UV radiation ranges from 100 to 400 nm, and ionizing radiation includes solar energetic particles (SEPs) and galactic cosmic rays (GCRs).

2.4.2.1 Ultraviolet Radiation

The UV spectrum is often divided into three ranges: UVA: 315–400 nm, UVB: 280–315 nm, and UVC: 100–280 nm. A second, also commonly used division is: near-UV: 300–400 nm, middle-UV: 200–300 nm; far-UV: 122–200 nm, Lyman-alpha radiation: 121–122 nm, and extreme UV: 10–121 nm. On Earth the ozone (O_3) layer, itself produced through UV-photodissociation of oxygen (O_2) and subsequent reaction of the produced molecular oxygen O with O_2 into O_3, absorbs most UVB radiation (but transmits just enough for vitamin D to be produced in primates) and all radiation with wavelengths shorter than that. Mars has no ozone layer and a thin, ca. 6 mbar atmosphere predominantly consisting of CO_2. CO_2 is transparent to wavelengths down to 190 nm, making UV radiation a factor to be considered. Several UV models exist, for varying zenith angles (Cockell, 2000), ancient Mars conditions at 3.5 Gyr ago (Molina-Cuberos, 2001), varying atmospheric dust loads (Patel et al., 2002) and aerosol content (Córdoba-Jabonero et al., 2003), and biological effects of these different UV scenarios (Rontó et al., 2003). The Rover Environmental Monitoring Station (REMS) onboard NASA's Curiosity rover provided the first UV measurements on the surface of Mars (Gómez-Elvira et al., 2012). REMS measures the total UV dose in six bands: 210–360 nm, 215–277 nm, 270–320 nm, 315–370 nm, 230–298 nm, and 311–343 nm, but due to the horizontal placement of the sensor on the rover deck, the sensor suffers from dust deposition, making correction of the measured data necessary (Vicente-Retortillo et al., 2020). The dust-corrected data suggest a daily 210–360 nm UV flux ranging from 9 W/m^2 at 7.00 local mean solar time (LMST) to 22 W/m^2 at noon, and back to 9 W/m^2 at 15.00 LMST (Vicente-Retortillo et al., 2020).

Many studies have focused on the effect of UV radiation on organic compounds on Mars, predominantly within the context of organic detection by missions such as Viking, Curiosity, Perseverance, and ExoMars. Exposure to UV for timescales up to 10 years will destroy organic compounds exposed on the surface (Dartnell et al., 2012; Dartnell & Patel, 2014; Poch et al., 2014; Stalport et al., 2009; ten Kate et al., 2005). This is merely a surface problem, as UV penetrates down to 500–1000 μm, depending on the mineral, but a layer of minerals thicker than 2 mm already has a nearly full shielding and protecting effect on the organic compounds (Ertem et al., 2017; Carrier et al., 2019). In addition to degrading or destructive effects on biological or meteoritic organic compounds, UV radiation also has damaging effects on a range of synthesized organic materials (plastics), including materials often used in spaceflight. For example, material properties including morphology, absorption, mechanical properties, and charge transport of polyimide, the material used as insulator in spacecraft, are affected by UV radiation (Plis et al., 2019). Depending on the wavelength and the dose, UV radiation could be deadly for microorganisms and harmful for organisms which are directly exposed. It is detrimental for some exposed organs (skin, retina, leaf…) of several species.

2.4.2.2 Ionizing Radiation

The ionizing radiation environment around Mars is dominated by GCRs and SEPs. GCRs are composed of ~2% electrons and 98% atomic nuclei, of which 87% are protons, 12% are Helium, and ~1% are heavier atoms ($Z \geq 3$) (Simpson, 1983). SEPs consist mainly of protons and electrons accelerated by solar eruptions, such as coronal mass ejections and flares. Mars lacks a magnetic field and has a very thin atmosphere, resulting in a surface exposed to nearly the full range of ionizing radiation, but variations occur due to heliospheric influences, Mars's atmospheric changes, topographical changes (Zhang et al., 2022), and solar particle events (Guo et al., 2019). Even though the Martian atmosphere is very tenuous, with a column depth of ~20 ± 5 g/cm^2, it still has a small shielding effect, causing primary particles to lose energy, but also causing secondary particles to be formed via spallation and fragmentation (Guo et al., 2019). The Radiation Assessment Detector (RAD) onboard the Curiosity Rover has made continuous radiation measurements since the launch of Curiosity in November 2011, first of the deep space radiation environment during the cruise phase and of the cosmic ray induced energetic particle radiation locally in Gale Crater since its landing on December 7, 2012 (See Sect. 7.4 for more information). The thickness of the Martian atmosphere and the composition of the surface material determine the fraction of particles reaching the surface and being able to penetrate. The composition of the regolith does influence the penetration depth to some extent, where pure ice transmits radiation down to 5 m and wet, hydrogen-rich regolith has slightly better shielding properties then dry regolith. The neutron flux and effective dose reach their maximum at around 30 cm depth, which is important both for the preservation of organic compounds and biosignatures (Dartnell et al., 2007; Alexander Pavlov et al., 2012, 2022) and for the use of Martian regolith as building material. For example, a maximum annual effective dose of 100 mSv requires a shielding depth of 80–250 cm.

The long-term preservation of chemical traces of putative early Martian life is only possible if they are shielded against ionizing radiation damage—that is, protected in the geological record underground at sufficient depth. Although the dose is not that high, its action over billions of years is deleterious and can degrade exposed bioorganic molecules beyond recognition.

2.5 Habitability and Potential for Extant Martian Life

The concept of habitability has been subject to many intense discussions within ecology, astrobiology, and planetary science. Rather than defining it just based on static environmental conditions, habitability should be regarded as a dynamic, complex function and interface of environmental conditions, space, geological timescales, and species type. Thus, according to Cockell et al. (2016), different categories of habitability can be distinguished, e.g., instantaneous habitability and continuous planetary habitability, and the nature of the habitability will also differ depending

on whether the considered astronomical body has surface liquid water (like Earth) or interior liquid water (such as icy moons or rocky planets with liquid water in the interior), and how available this water is—as availability may be reduced due to hypersaline conditions (Cockell et al., 2016). Further, that an astronomical body may be habitable does not automatically imply that it contains (or contained) life. Where does Mars fit within these concepts? The Mars of today is generally regarded as hostile due to high radiation, lack of magnetic field, microgravity, dust storms, meteorite or asteroid falls, toxic compounds in soils and bedrock, and other tough conditions, as described above in more detail (Checinska Sielaff & Smith, 2019). However, Mars does have reservoirs of water, oxygen could be produced from local sources, elements important for life such as phosphorus and nitrogen are present in the soil, elements and compounds used in construction materials such as iron and clay are available, and there are even protective sites such as caves in the subsurface. Further chapters will analyse whether those resources may be used by humans and the terrestrial life forms they will bring with them to survive on Mars for a long time period. Could advance in research and technology truly overcome all the hostile conditions as outlined in other chapters?.

Mars is a planet of great interest in the search for signatures of past or present life beyond Earth. The years of research, and more advanced instrumentation, have yielded a lot of evidence which may be considered by the scientific community as proof of past or present habitability of Mars. Recent discoveries including seasonal methane releases and a subglacial lake are exciting, yet challenging findings. Concurrently, laboratory and environmental studies on the limits of microbial life in extreme environments on Earth broaden our knowledge of the possibility of Mars habitability. In this review, we aim to: (1) discuss the characteristics of the Martian surface and subsurface that may be conducive to habitability either in the past or at present; (2) discuss laboratory-based studies on Earth that provide us with discoveries on the limits of life; and (3) summarize the current state of knowledge in terms of direction for future research (Checinska Sielaff & Smith, 2019). The field of astrobiology aims to understand the origin of life on Earth and searches for evidence of life beyond our planet. Although there is agreement on some of the requirements for life on Earth, the exact process by which life emerged from prebiotic conditions is still uncertain, leading to various theories. In order to expand our knowledge of life and our place in the universe, scientists look for signs of life through the use of biosignatures, observations that suggest the presence of past or present life. These biosignatures often require up-close investigation by orbiters and landers, which have been employed in various space missions. Mars, because of its proximity and Earth-like environment, has received the most attention and has been explored using (sub)surface sampling and analysis. Despite its inhospitable surface conditions, Venus has also been the subject of space missions due to the presence of potentially habitable conditions in its atmosphere. In addition, the discovery of habitable environments on icy moons has sparked interest in further study. This part of chapter 2 provides an overview of the origin of life on Earth and the astrobiology studies carried out by orbiters and landers (De Mol, 2023). Data

collected from recent spacecraft missions to Mars are making it possible to scientifically evaluate whether habitable environments are present, or existed in the past, on the planet. Determining where, when, and how such environments occur will play a crucial role in guiding future exploration efforts. Mars appears to possess the critical elements for life as we know it, including the required chemical elements, energy sources, and the presence of water. Identification of potential habitats for life therefore depends on the convergence of these factors under favourable circumstances. Spacecraft observations are more clearly defining the history of water on Mars and appear to indicate that significant amounts of liquid water have been present at the surface in the past. Most of this water has been lost over time or retreated underground, although there is some evidence for periodic near-surface water in particular eras. If Mars did indeed have a warmer, wetter past, the possibilities for habitable environments were substantial and diverse. On the other hand, the inhospitable nature of the present surface indicates that potential habitats for extant life are much more limited. Nevertheless, habitable environments might exist in the subsurface or at the surface during more favourable climatic periods (McCollom, 2006). Recent findings suggest that Mars was more habitable in the past because of the presence of liquid water on the surface, as demonstrated by morphological, mineralogical, and chemical analyses. Several potential sites have been identified as ancient habitable environments including Gale and Jezero Crater (explored by the Curiosity and Perseverance rovers) and potentially caves or/and the subsurface (Checinska Sielaff & Smith, 2019; De Mol, 2023; McCollom, 2006; 'NASA Astrobiology', 2023). On Earth, the subsurface is a target site for research on extreme microbial life forms which are independent of solar energy and other resources available on Earth's surface (e.g. Suzuki et al., 2022). Some of these extremophiles, which largely remain uncharacterized, have played an important role for virtually all biogeochemical processes throughout Earth's history, providing essential support to many life forms on Earth surface, for instance by altering the composition of minerals and groundwater. In fact, these microbes are even assumed to make up a large part of all life forms on Earth, and they have been found on next to all types of subsurface systems, including marine sediments and the terrestrial subsurface (bedrock pores and veins, where the geological processes strongly influenced the selection within the populations and their evolution).

The most likely life forms to be found on Mars would be or have been polyextremophilic (i.e. tolerant to multiple extreme conditions) microorganisms because of the multiple extreme environmental factors there (Westall et al., 2013) (Table 2.2). Several types of metabolism that exist on Earth have been suggested to be compatible with the sourcing of nutrients and energy on Mars, such as those of metal cyclers or methanogens (Sauterey et al., 2022; Nixon et al., 2013). However, the question is whether current technology is sufficient to detect these, considering a number of foreseeable biases such as sampling technique (depth, volume), sampling location, preservation issues of samples prior to analyses, and the detection method used (Westall et al., 2015).

The question of whether extinct or extant life can be found on Mars is tightly connected to these pertaining to human exploration. Part of the reason for this

Table 2.2 Overview of extremophile categories whose features could help survival (or even proliferation) on Mars. Adapted from Merino et al. (2019)

Category of extremophiles	Organisms that can grow and reproduce	Example of taxa on Earth
Anaerobes	Without atmospheric oxygen	Many species within Archaea, Bacteria, and some Eukaryotes
Acidophiles	In low pH	Many species within Archaea, Bacteria, and some Eukaryotes
Cryptoendoliths	In rocks (pores, fissures)	Many species within Archaea, Bacteria, and some Eukaryotes
Hypoliths	Beneath rocks in cold deserts	Many species within Archaea, Bacteria, and some Eukaryotes
Osmophiles	With high osmotic pressures, e.g. high sugar or salt concentrations	Several species among fungi (yeast) and bacteria
Oligotrophs	In low nutrient concentrations	Many species within Archaea, Bacteria and some Eukaryotes
Psychrophiles	Under low temperatures	Many species within Archaea, Bacteria, Eukaryotes (lichens, algae, plankton, fungi, insects)
Radioresistant	Under high dose rates of ionizing radiation, including nuclear radiation	Some species within Archaea, Bacteria, and some Eukaryotes
Sulphophile	With high concentrations of sulfur	Sulfur-oxidizing and sulfur-reducing species.
Xerophiles	Under a low water activity (a_w)	Bacteria: *Bacillus* spp., *Clostridium* spp., *Salmonella* spp. Fungi: *Aspergillus* spp., *Penicillium* spp., *Xeromyces* spp., *Zygosaccharomyces* spp.

comes from potential risks to planetary protection: indigenous life forms on Mars must be protected from humans and vice versa (for more details, see Sect. 4.5).

2.6 Take-Home Message

Mars, the third closest planet to Earth, formed at approximately the same time: about 4.6 billion years ago. It has since undergone a complex geological evolution. Four billion years ago, the environmental conditions were probably warm and wet enough to be supportive of prebiotic chemistry. A dramatic climate change later made Mars inhospitable: it turned into a dry, cold planet with a thin atmosphere. Scientifically, several questions remain open on the origin and evolution of Mars, and on potential development of life; answering them requires further exploration.

Robotic missions have demonstrated that Mars's environmental conditions are, by comparison with the other non-Earth planets of the Solar System, benign. These conditions seem compatible with the preservation of traces of putative life forms from the past. It also cannot be ruled out that life exists somewhere on Mars today.

After robotic investigations, a logical next step would be to explore Mars with crewed spacecraft. Mars is the most distant celestial body which human explorers can expect to reach with today's or tomorrow's, technologies. An abundant literature therefore promises a bright future for Mars exploration, or even settlement. Some local resources have been identified which could be used for long stays or to supply a permanent base. Before such human missions can become reality, however, many obstacles remain to be overcome and knowledge gaps to be filled.

References

Acuña, M. H., Connerney, J. E. P., Ness, F. N., Lin, R. P., Mitchell, D., Carlson, C. W., McFadden, J., et al. (1999). Global distribution of crustal magnetization discovered by the mars global surveyor MAG/ER experiment. *Science, 284*(5415), 790–793. https://doi.org/10.1126/science.284.5415.790

Adcock, C. T., Hausrath, E. M., & Forster, P. M. (2013). Readily available phosphate from minerals in early aqueous environments on Mars. *Nature Geoscience, 6*(10), 824–827. https://doi.org/10.1038/ngeo1923

Agee, C. B., Wilson, N. V., McCubbin, F. M., Ziegler, K., Polyak, V. J., Sharp, Z. D., Asmerom, Y., et al. (2013). Unique meteorite from early Amazonian Mars: Water-rich Basaltic Breccia Northwest Africa 7034. *Science, 339*(6121), 780–785. https://doi.org/10.1126/science.1228858

Artemieva, N., & Ivanov, B. (2004). Launch of Martian meteorites in oblique impacts. *Icarus, 171*(1), 84–101. https://doi.org/10.1016/j.icarus.2004.05.003

Balme, M., & Greeley, R. (2006). Dust devils on earth and mars. *Reviews of Geophysics, 44*(3), 2005RG000188. https://doi.org/10.1029/2005RG000188

Bandfield, J. L., Hamilton, V. E., & Christensen, P. R. (2000). A global view of Martian surface compositions from MGS-TES. *Science, 287*(5458), 1626–1630. https://doi.org/10.1126/science.287.5458.1626

Banerdt, W. B., Smrekar, S., Banfield, D., & the InSight Team. (2020). Initial results from the InSight mission on Mars. *Nature Geoscience, 13*, 183–189. https://doi.org/10.1038/s41561-020-0544-y

Baratoux, D., Samuel, H., Michaut, C., Toplis, M. J., Monnereau, M., Wieczorek, M., Garcia, R., & Kurita, K. (2014). Petrological constraints on the density of the Martian crust. *Journal of Geophysical Research: Planets, 119*(7), 1707–1727. https://doi.org/10.1002/2014JE004642

Barnes, J. J., McCubbin, F. M., Santos, A. R., et al. (2020). Multiple early-formed water reservoirs in the interior of Mars. *Nature Geoscience, 13*, 260–264. https://doi.org/10.1038/s41561-020-0552-y

Bibring, J.-P., Langevin, Y., Mustard, J. F., Poulet, F., Arvidson, R., Gendrin, A., Gondet, B., et al. (2006). Global mineralogical and aqueous Mars history derived from OMEGA/Mars express data. *Science, 312*(5772), 400–404. https://doi.org/10.1126/science.1122659

Bish, D. L., Blake, D. F., Vaniman, D. T., Chipera, S. J., Morris, R. V., Ming, D. W., Treiman, A. H., et al. (2013). X-ray diffraction results from Mars Science Laboratory: Mineralogy of rocknest at Gale Crater. *Science, 341*(6153), 1238932. https://doi.org/10.1126/science.1238932

Borin, P., Cremonese, G., Marzari, F., & Lucchetti, A. (2017). Asteroidal and cometary dust flux in the inner solar system. *Astronomy & Astrophysics, 605*(September), A94. https://doi.org/10.1051/0004-6361/201730617

Bottke, W. F., & Andrews-Hanna, J. C. (2017). A post-accretionary lull in large impacts on early Mars. *Nature Geoscience, 10*(5), 344–348. https://doi.org/10.1038/ngeo2937

Boynton, W. V., Taylor, G. J., Evans, L. G., Reedy, R. C., Starr, R., Janes, D. M., Kerry, K. E., et al. (2007). Concentration of H, Si, Cl, K, Fe, and Th in the low- and mid-latitude regions of Mars. *Journal of Geophysical Research: Planets, 112*(E12), 2007JE002887. https://doi.org/10.1029/2007JE002887

Bramson, A. M., Byrne, S., Putzig, N. E., Sutton, S., Plaut, J. J., Charles Brothers, T., & Holt, J. W. (2015). Widespread excess ice in Arcadia Planitia, Mars. *Geophysical Research Letters, 42*(16), 6566–6574. https://doi.org/10.1002/2015GL064844

Broquet, A., & Andrews-Hanna, J. C. (2022). Geophysical evidence for an active mantle plume underneath Elysium Planitia on Mars. *Nature Astronomy, 7*, 160–169. https://doi.org/10.1038/s41550-022-01836-3

Burt, D. M., Knauth, L. P., & Wohletz, K. H. (2008). The late heavy bombardment: Possible influence on Mars. *Early Solar System Impact Bombardment, 1439*, 23–24.

Byrne, S., Dundas, C. M., Kennedy, M. R., Mellon, M. T., McEwen, A. S., Cull, S. C., Daubar, I. J., et al. (2009). Distribution of mid-latitude ground ice on Mars from new impact craters. *Science, 325*(5948), 1674–1676. https://doi.org/10.1126/science.1175307

Carr, M. H. (2007). *The surface of Mars*. Cambridge Planetary Science. Cambridge University Press. https://doi.org/10.1017/CBO9780511536007.

Carr, M. H., & Head, J. W. (2010). Geologic history of Mars. *Earth and Planetary Science Letters, 294*(3), 185–203. https://doi.org/10.1016/j.epsl.2009.06.042

Carr, M., & Head, J. (2019). Mars: formation and fate of a frozen Hesperian Ocean. *Icarus, 319*(February), 433–443. https://doi.org/10.1016/j.icarus.2018.08.021

Carrier, B. L., Abbey, W. J., Beegle, L. W., Bhartia, R., & Liu, Y. (2019). Attenuation of ultraviolet radiation in rocks and minerals: Implications for Mars science. *Journal of Geophysical Research: Planets, 124*(10), 2599–2612. https://doi.org/10.1029/2018JE005758

Carter, J., & Poulet, F. (2013). Ancient Plutonic processes on Mars inferred from the detection of possible Anorthositic Terrains. *Nature Geoscience, 6*(12), 1008–1012. https://doi.org/10.1038/ngeo1995

Carter, J., Loizeau, D., Mangold, N., Poulet, F., & Bibring, J.-P. (2015). Widespread surface weathering on early Mars: A case for a warmer and wetter climate. *Icarus, 248*(March), 373–382. https://doi.org/10.1016/j.icarus.2014.11.011

Checinska Sielaff, A., & Smith, S. A. (2019). Habitability of Mars: How welcoming are the surface and subsurface to life on the red planet? *Geosciences, 9*(9), 361. https://doi.org/10.3390/geosciences9090361

Chipera, S. J., Vaniman, D. T., Rampe, E. B., Bristow, T. F., Martínez, G., Tu, V. M., Peretyazhko, T. S., et al. (2023). Mineralogical investigation of Mg-sulfate at the Canaima Drill Site, Gale Crater, Mars. *Journal of Geophysical Research: Planets, 128*(11), e2023JE008041. https://doi.org/10.1029/2023JE008041

Clancy, R. T., Sandor, B. J., Wolff, M. J., Christensen, P. R., Smith, M. D., Pearl, J. C., Conrath, B. J., & Wilson, R. J. (2000). An intercomparison of ground-based millimeter, MGS TES, and Viking atmospheric temperature measurements: seasonal and interannual variability of temperatures and dust loading in the global Mars atmosphere. *Journal of Geophysical Research, 105*, 9553–9572.

Cockell, C. (2000). The ultraviolet environment of Mars: Biological implications past, present, and future. *Icarus, 146*(2), 343–359. https://doi.org/10.1006/icar.2000.6393

Cockell, C. S., Bush, T., Bryce, C., Direito, S., Fox-Powell, M., Harrison, J. P., Lammer, H., et al. (2016). Habitability: A review. *Astrobiology, 16*(1), 89–117. https://doi.org/10.1089/ast.2015.1295

Connerney, J. E. P., Acuña, M. H., Ness, N. F., et al. (2005). Tectonic implications of Mars Crustal Magnetism. *Proceedings of the National Academy of Sciences, 102*(42), 14970–14975. https://doi.org/10.1073/pnas.0507469102

Connerney, J. E. P., Acuña, M. H., Wasilewski, P. J., et al. (1999). Magnetic lineations in the ancient crust of Mars. *Science, 284*(5415), 794–798. https://doi.org/10.1126/science.284.5415.794

Córdoba-Jabonero, C., Lara, L. M., Mancho, A. M., Márquez, A., & Rodrigo, R. (2003). Solar ultraviolet transfer in the Martian atmosphere: Biological and geological implications. *Planetary and Space Science, 51*(6), 399–410. https://doi.org/10.1016/S0032-0633(03)00023-0

Corpolongo, A., Jakubek, R. S., Burton, A. S., Brown, A. J., Yanchilina, A., Czaja, A. D., Steele, A., et al. (2023). SHERLOC Raman mineral class detections of the Mars 2020 crater floor campaign. *Journal of Geophysical Research: Planets, 128*(3), e2022JE007455. https://doi.org/10.1029/2022JE007455

Crismani, M. M. J., Schneider, N. M., Plane, J. M. C., Evans, J. S., Jain, S. K., Chaffin, M. S., Carrillo-Sanchez, J. D., et al. (2017). Detection of a persistent meteoric metal layer in the Martian atmosphere. *Nature Geoscience, 10*(6), 401–404. https://doi.org/10.1038/ngeo2958

Dartnell, L. R., Desorgher, L., Ward, J. M., & Coates, A. J. (2007). Modelling the surface and subsurface Martian radiation environment: Implications for astrobiology. *Geophysical Research Letters, 34*(2), 2006GL027494. https://doi.org/10.1029/2006GL027494

Dartnell, L. R., & Patel, M. R. (2014). Degradation of microbial fluorescence biosignatures by solar ultraviolet radiation on Mars. *International Journal of Astrobiology, 13*(2), 112–123. https://doi.org/10.1017/S1473550413000335

Dartnell, L. R., Patel, M. R., Storrie-Lombardi, M. C., Ward, J. M., & Muller, J.-P. (2012). Experimental determination of photostability and fluorescence-based detection of PAHs on the Martian surface. *Meteoritics & Planetary Science, 47*(5), 806–819. https://doi.org/10.1111/j.1945-5100.2012.01351.x

David, G., Dehouck, E., Meslin, P.-Y., Rapin, W., Cousin, A., Forni, O., Gasnault, O., et al. (2022). Evidence for amorphous sulfates as the main carrier of soil hydration in Gale Crater, Mars. *Geophysical Research Letters, 49*(21), e2022GL098755. https://doi.org/10.1029/2022GL098755

De Mol, M. L. (2023). Astrobiology in space: A comprehensive look at the solar system. *Life, 13*(3), 675. https://doi.org/10.3390/life13030675

Dehouck, E., Mangold, N., Le Mouélic, S., Ansan, V., & Poulet, F. (2010). Ismenius Cavus, Mars: A deep paleolake with phyllosilicate deposits. *Planetary and Space Science, 58*(6), 941–946. https://doi.org/10.1016/j.pss.2010.02.005

Dickson, J. L., Head, J. W., Levy, J. S., & Marchant, D. R. (2013). Don Juan Pond, Antarctica: Near-surface CaCl2-brine feeding earth's most saline lake and implications for Mars. *Scientific Reports, 3*(1), 1166. https://doi.org/10.1038/srep01166

Dietrich, W., & Wicht, J. (2013). A hemispherical dynamo model: Implications for the Martian crustal magnetization. *Physics of the Earth and Planetary Interiors, 217*, 10–21. https://doi.org/10.1016/j.pepi.2013.01.001

Dundas, C. M., Bramson, A. M., Ojha, L., Wray, J. J., Mellon, M. T., Byrne, S., McEwen, A. S., et al. (2018). Exposed subsurface ice sheets in the Martian mid-latitudes. *Science, 359*(6372), 199–201. https://doi.org/10.1126/science.aao1619

Ehlmann, B. L., Berger, G., Mangold, N., Michalski, J. R., Catling, D. C., Ruff, S. W., Chassefière, E., Niles, P. B., Chevrier, V., & Poulet, F. (2013). Geochemical consequences of widespread clay mineral formation in Mars' ancient crust. *Space Science Reviews, 174*(1–4), 329–364. https://doi.org/10.1007/s11214-012-9930-0

Ehlmann, B. L., & Edwards, C. S. (2014). Mineralogy of the Martian surface. *Annual Review of Earth and Planetary Sciences, 42*(1), 291–315. https://doi.org/10.1146/annurev-earth-060313-055024

Eichler, A., Hadland, N., Pickett, D., Masaitis, D., Handy, D., Perez, A., Batcheldor, D., Wheeler, B., & Palmer, A. (2021). Challenging the agricultural viability of Martian regolith simulants. *Icarus, 354*(January), 114022. https://doi.org/10.1016/j.icarus.2020.114022

Eigenbrode, J. L., Summons, R. E., Steele, A., Freissinet, C., Millan, M., Navarro-González, R., Sutter, B., et al. (2018). Organic matter preserved in 3-billion-year-old mudstones at Gale Crater, Mars. *Science, 360*(6393), 1096–1101. https://doi.org/10.1126/science.aas9185

Elkins-Tanton, L. T. (2012). Magma Oceans in the inner solar system. *Annual Review of Earth and Planetary Sciences, 40*, 113–139. https://doi.org/10.1146/annurev-earth-042711-105503

Ertem, G., Ertem, M. C., McKay, C. P., & Hazen, R. M. (2017). Shielding biomolecules from effects of radiation by Mars analogue minerals and soils. *International Journal of Astrobiology, 16*(3), 280–285. https://doi.org/10.1017/S1473550416000331

Farley, K. A., & Stack, K. M. (2023). *Mars 2020 initial reports* (Vol. 2) (Samples 11-21). Delta Front Campaign. https://doi.org/10.17189/49zd-2k55.

Fernando, B., Daubar, I. J., Charalambous, C., Grindrod, P. M., Stott, A., Al Ateqi, A., Atri, D., et al. (2023). A tectonic origin for the largest marsquake observed by InSight. *Geophysical Research Letters, 50*(20), e2023GL103619. https://doi.org/10.1029/2023GL103619

Fischer, E., Martínez, G. M., Rennó, N. O., Tamppari, L. K., & Zent, A. P. (2019). Relative humidity on Mars: New results from the phoenix TECP sensor. *Journal of Geophysical Research: Planets, 124*(11), 2780–2792. https://doi.org/10.1029/2019JE006080

Formisano, V., Atreya, S., Encrenaz, T., Ignatiev, N., & Giuranna, M. (2004). Detection of methane in the atmosphere of Mars. *Science, 306*(5702), 1758–1761. https://doi.org/10.1126/science.1101732

Foss, F. J., Putzig, N. E., Campbell, B. A., & Phillips, R. J. (2017). 3-D imaging of Mars' polar ice caps using orbital radar data. *Leading Edge (Tulsa, Okla.: Online), 36*(1), 43–57. https://doi.org/10.1190/tle36010043.1

Frantseva, K., Mueller, M., Ten Kate, I. L., Van Der Tak, F. F. S., & Greenstreet, S. (2018). Delivery of organics to Mars through asteroid and comet impacts. *Icarus, 309*(July), 125–133. https://doi.org/10.1016/j.icarus.2018.03.006

Freissinet, C., Glavin, D. P., Mahaffy, P. R., Miller, K. E., Eigenbrode, J. L., Summons, R. E., Brunner, A. E., et al. (2015). Organic molecules in the sheepbed mudstone, Gale Crater, Mars. *Journal of Geophysical Research: Planets, 120*(3), 495–514. https://doi.org/10.1002/2014JE004737

Frey, H. V. (2006). Impact constraints on the age and origin of the lowlands of Mars. *Geophysical Research Letters, 33*(8), L08S02. https://doi.org/10.1029/2005GL024484

Frydenvang, J., Mangold, N., Wiens, R. C., Fraeman, A. A., Edgar, L. A., Fedo, C. M., L'Haridon, J., et al. (2020). The chemostratigraphy of the Murray formation and role of diagenesis at Vera Rubin Ridge in Gale Crater, Mars, as observed by the ChemCam Instrument. *Journal of Geophysical Research: Planets, 125*(9), e2019JE006320. https://doi.org/10.1029/2019JE006320

Fuentes-Muñoz, O., Scheeres, D. J., Farnocchia, D., & Park, R. S. (2023). The hazardous Km-Sized NEOs of the next thousands of years. *The Astronomical Journal, 166*(1), 10. https://doi.org/10.3847/1538-3881/acd378

Fuller, E. R., & Head, J. W., III. (2002). Amazonis Planitia: The role of geologically recent volcanism and sedimentation in the formation of the smoothest plains on Mars. *Journal of Geophysical Research: Planets, 107*(E10), 11-1–11-25. https://doi.org/10.1029/2002JE001842

Garcia, R. F., Daubar, I. J., Beucler, É., Posiolova, L. V., Collins, G. S., Lognonné, P., Rolland, L., et al. (2022). Newly formed craters on Mars located using seismic and acoustic wave data from InSight. *Nature Geoscience, 15*(10), 774–780. https://doi.org/10.1038/s41561-022-01014-0

Gendrin, A., Mangold, N., Bibring, J.-P., Langevin, Y., Gondet, B., Poulet, F., Bonello, G., et al. (2005). Sulfates in Martian layered terrains: The OMEGA/Mars express view. *Science, 307*(5715), 1587–1591. https://doi.org/10.1126/science.1109087

Genova, A., Goossens, S., Lemoine, F. G., Mazarico, E., Neumann, G. A., Smith, D. E., & Zuber, M. T. (2016). Seasonal and static gravity field of Mars from MGS, Mars Odyssey and MRO radio science. *Icarus, 272*, 228–245. https://doi.org/10.1016/j.icarus.2016.02.050

Giardini, D., Lognonné, P., Banerdt, W. B., Pike, W. T., Christensen, U., Ceylan, S., Clinton, J. F., et al. (2020). The seismicity of Mars. *Nature Geoscience, 13*(3), 205–212. https://doi.org/10.1038/s41561-020-0539-8

Gómez-Elvira, J., Armiens, C., Castañer, L., Domínguez, M., Genzer, M., Gómez, F., Haberle, R., et al. (2012). REMS: The environmental sensor suite for the Mars Science Laboratory Rover. *Space Science Reviews, 170*(1–4), 583–640. https://doi.org/10.1007/s11214-012-9921-1

Grady, M. M., Summons, R. E., Swindle, T. D., Westall, F., Kminek, G., Meyer, M. A., Beaty, D. W., et al. (2022). The scientific importance of returning airfall dust as a part of Mars Sample Return (MSR). *Astrobiology, 22*(S1), S-176–S-185. https://doi.org/10.1089/ast.2021.0111

Gunell, H., Maggiolo, R., Nilsson, H., Stenberg, W. G., Slapak, R., Lindkvist, J., Hamrin, M., & De Keyser, J. (2018). Why an intrinsic magnetic field does not protect a planet against atmospheric escape? *Astronomy & Astrophysics, 614*(L3), 1–8. https://doi.org/10.1051/0004-6361/201832934

Guo, J., Wimmer-Schweingruber, R. F., Grande, M., Lee-Payne, Z. H., & Matthia, D. (2019). Ready functions for calculating the Martian radiation environment. *Journal of Space Weather and Space Climate, 9*, A7. https://doi.org/10.1051/swsc/2019004

Guzewich, S. D., Toigo, A. D., & Wang, H. (2017). An investigation of dust storms observed with the Mars color imager. *Icarus, 289*(June), 199–213. https://doi.org/10.1016/j.icarus.2017.02.020

Haberle, R. M., Todd Clancy, R., Forget, F., Smith, M. D., & Zurek, R. W. (Eds.). (2017). *The atmosphere and climate of Mars*. Cambridge Planetary Science 18. Cambridge University Press.

Hauber, E., Broz, P., Jagert, F., Jodłowski, P., & Platz, T. (2011). Very recent and wide-spread basaltic volcanism on Mars. *Geophysical Research Letters, 38*(L10201). https://doi.org/10.1029/2011GL047310

Hausrath, E. M., Adcock, C. T., Bechtold, A., Beck, P., Benison, K., Brown, A., Cardarelli, E. L., et al. (2023). An examination of soil crusts on the floor of Jezero Crater, Mars. *Journal of Geophysical Research: Planets, 128*(10), e2022JE007433. https://doi.org/10.1029/2022JE007433

Head, J. W., Wilson, L., & Weitz, C. M. (2002). Dark ring in southwestern orientale basin: Origin as a single pyroclastic eruption. *Journal of Geophysical Research: Planets, 107*(E1). https://doi.org/10.1029/2000JE001438

Hecht, M. H., Kounaves, S. P., Quinn, R. C., West, S. J., Young, S. M. M., Ming, D. W., Catling, D. C., et al. (2009). Detection of perchlorate and the soluble chemistry of Martian soil at the Phoenix Lander Site. *Science, 325*(5936), 64–67. https://doi.org/10.1126/science.1172466

Holsapple, K. A. (1993). The scaling of impact processes in planetary sciences. *Annual Review of Earth and Planetary Sciences, 21*(1), 333–373. https://doi.org/10.1146/annurev.ea.21.050193.002001

Holsapple, K. A., & Housen, K. R. (2007). A crater and its ejecta: An interpretation of deep impact. *Icarus, 191*(2), 586–597. https://doi.org/10.1016/j.icarus.2006.08.035

Holt, J. W., Safaeinili, A., Plaut, J. J., Head, J. W., Phillips, R. J., Seu, R., Kempf, S. D., et al. (2008). Radar sounding evidence for buried glaciers in the southern mid-latitudes of Mars. *Science, 322*(5905), 1235–1238. https://doi.org/10.1126/science.1164246

Hood, L. L., Richmond, N. C., Pierazzo, E., & Rochette, P. (2003). Distribution of crustal magnetic fields on Mars: Shock effects of basin-forming impacts. *Geophysical Research Letters, 30*(6), 1281. https://doi.org/10.1029/2002GL016657

Horvath, D. G., Moitra, P., Hamilton, C. W., Craddock, R. A., & Andrews-Hanna, J. C. (2021). Evidence for geologically recent explosive volcanism in Elysium Planitia, Mars. *Icarus, 365*, 114499. https://doi.org/10.1016/j.icarus.2021.114499

Hörz, F., Hartung, J. B., & Gault, D. E. (1971). Micrometeorite craters and related features on lunar rock surfaces. *Earth and Planetary Science Letters, 10*(4), 381–386. https://doi.org/10.1016/0012-821X(71)90084-7

Humayun, M., Nemchin, A., Zanda, B., Hewins, R. H., Grange, M., Kennedy, A., Lorand, J.-P., et al. (2013). Origin and age of the earliest Martian crust from meteorite NWA 7533. *Nature, 503*(7477), 513–516. https://doi.org/10.1038/nature12764

Ivanov, B. A. (2001). Mars/Moon cratering rate ratio estimates. *Space Science Reviews, 96*(1/4), 87–104. https://doi.org/10.1023/A:1011941121102

Janches, D., Nolan, M. C., Meisel, D. D., Mathews, J. D., Zhou, Q. H., & Moser, D. E. (2003). On the geocentric micrometeor velocity distribution. *Journal of Geophysical Research: SpacePhysics, 108*(A6), 2002JA009789. https://doi.org/10.1029/2002JA009789

Kate, I. L., Garry, J. R. C., Peeters, Z., Quinn, R., Foing, B., & Ehrenfreund, P. (2005). Amino acid photostability on the Martian surface. *Meteoritics & Planetary Science, 40*(8), 1185–1193. https://doi.org/10.1111/j.1945-5100.2005.tb00183.x

Khan, A., Huang, D., Durán, C., Sossi, P. A., Giardini, D., & Murakami, M. (2023). Evidence for a liquid silicate layer atop the Martian core. *Nature, 622*(7984), 718–723. https://doi.org/10.1038/s41586-023-06586-4

Khan, A., Ceylan, S., Van Driel, M., Giardini, D., Lognonné, P., Samuel, H., Schmerr, N. C., et al. (2021). Upper mantle structure of Mars from InSight seismic data. *Science, 373*(6553), 434–438. https://doi.org/10.1126/science.abf2966

Kim, D., Duran, C., Giardini, D., Plesa, A.-C., Stähler, S. C., Boehm, C., Lekić, V., et al. (2023). Global crustal thickness revealed by surface waves orbiting Mars. *Geophysical Research Letters, 50*(12), e2023GL103482. https://doi.org/10.1029/2023GL103482

Knapmeyer-Endrun, B., Panning, M. P., Bissig, F., Joshi, R., Khan, A., Kim, D., Lekić, V., et al. (2021). Thickness and structure of the Martian crust from InSight seismic data. *Science, 373*(6553), 438–443. https://doi.org/10.1126/science.abf8966

Konopliv, A. S., Park, R. S., & Folkner, W. M. (2016). An improved JPL Mars gravity field and orientation from Mars orbiter and lander tracking data. *Icarus, 274*, 253–260. https://doi.org/10.1016/j.icarus.2016.02.052

Konopliv, A. S., Park, R. S., Folkner, W. M., Rivoldini, A., Baland, R.-M., Le Maistre, S., Van Hoolst, T., Yseboodt, M., & Dehant, V. (2020). Detection of the Mars Chandler Wobble from Mars orbiting spacecraft. *Geophysical Research Letters, 47*, e2020GL090568. https://doi.org/10.1029/2020GL090568

Korablev, O., Vandaele, A. C., Montmessin, F., Fedorova, A. A., Trokhimovskiy, A., Forget, F., Lefèvre, F., et al. (2019). No detection of methane on Mars from early ExoMars trace gas orbiter observations. *Nature, 568*(7753), 517–520. https://doi.org/10.1038/s41586-019-1096-4

Kruijer, T. S., Borg, L. E., Wimpenny, J., & Sio, C. K. (2020). Onset of Magma Ocean solidification on Mars inferred from Mn-Cr chronometry. *Earth and Planetary Science Letters, 542*, 116315. https://doi.org/10.1016/j.epsl.2020.116315

Lammer, H. (2013). *Origin and evolution of planetary atmospheres: Implications for habitability*. Briefs in Astronomy. Springer.

Lasue, J., Clifford, S. M., Conway, S. J., Mangold, N., & Butcher, F. E. G. (2019). The hydrology of Mars including a potential cryosphere. In *Volatiles in the Martian Crust* (pp. 185–246). Elsevier. https://doi.org/10.1016/B978-0-12-804191-8.00007-6

Le Maistre, S., Caldiero, A., Rivoldini, A., Yseboodt, M., Baland, R.-M., Beuthe, M., Van Hoolst, T., Dehant, V., Folkner, W. M., et al. (2023). Spin state and deep interior structure of Mars from InSight radio tracking. *Nature*. https://doi.org/10.1038/s41586-023-06150-0

Lee, N. M., Meisinger, D. B., Aubrecht, R., Kovacik, L., Saiz-Jimenez, C., Baskar, S., Baskar, R., Liebl, W., Porter, M. L., & Engel, A. S. (2012). Caves and karst environments. In E. M. Bell (Ed.), *Life at extremes: Environments, organisms and strategies for survival* (1st ed., pp. 320–344). CABI. https://doi.org/10.1079/9781845938147.0320

Lillis, R. J., Frey, H. V., & Manga, M. (2008a). Rapid decrease in Martian crustal magnetization in the Noachian era: Implications for the dynamo and climate of early Mars. *Geophysical Research Letters, 35*, L14203. https://doi.org/10.1029/2008GL034338

Lillis, R. J., Frey, H. V., Manga, M., Mitchell, D. L., Lin, R. P., Acuña, M. H., & Bougher, S. W. (2008b). An improved crustal magnetic field map of Mars from electron reflectometry: Highland volcano magmatic history and the end of the Martian dynamo. *Icarus, 194*(2), 575–596. https://doi.org/10.1016/j.icarus.2007.09.032

Mangold, N., Thompson, L. M., Forni, O., Williams, A. J., Fabre, C., Le Deit, L., Wiens, R. C., et al. (2016). Composition of conglomerates analyzed by the Curiosity Rover: Implications

for Gale crater crust and sediment sources. *Journal of Geophysical Research: Planets, 121*(3), 353–387. https://doi.org/10.1002/2015JE004977

Marty, J. C., Balmino, G., Duron, J., Rosenblatt, P., Le Maistre, S., Rivoldini, A., Dehant, V., & Van Hoolst, T. (2009). Martian gravity field model and its time variations from MGS and Odyssey data. *Planetary and Space Science, 57*(3), 350–363. https://doi.org/10.1016/j.pss.2009.01.004

McCollom, T. M. (2006). The habitability of Mars: Past and present. In P. Blondel & J. W. Mason (Eds.), *Solar system update* (pp. 159–175). Springer Praxis Books. https://doi.org/10.1007/3-540-37683-6_6

McSween Jr, H. Y., & Treiman, A. H. (1998). Chapter 6. MARTIAN METEORITES. In J. J. Papike (Ed.), *Planetary materials* (pp. 953–1006). De Gruyter. https://doi.org/10.1515/9781501508806-021

Meech, K. J., Hainaut, O. R., & Marsden, B. G. (2004). Comet nucleus size distributions from HST and Keck telescopes. *Icarus, 170*(2), 463–491. https://doi.org/10.1016/j.icarus.2004.03.014

Merino, N., Aronson, H. S., Bojanova, D. P., Feyhl-Buska, J., Wong, M. L., Zhang, S., & Giovannelli, D. (2019). Living at the extremes: Extremophiles and the limits of life in a planetary context. *Frontiers in Microbiology, 10*(April), 780. https://doi.org/10.3389/fmicb.2019.00780

Millan, M., Teinturier, S., Malespin, C. A., Bonnet, J. Y., Buch, A., Dworkin, J. P., Eigenbrode, J. L., et al. (2021). Organic molecules revealed in Mars's Bagnold Dunes by Curiosity's derivatization experiment. *Nature Astronomy, 6*(1), 129–140. https://doi.org/10.1038/s41550-021-01507-9

Millan, M., Williams, A. J., McAdam, A. C., Eigenbrode, J. L., Steele, A., Freissinet, C., Glavin, D. P., et al. (2022). Sedimentary organics in Glen Torridon, Gale Crater, Mars: Results from the SAM instrument suite and supporting laboratory analyses. *Journal of Geophysical Research: Planets, 127*(11), e2021JE007107. https://doi.org/10.1029/2021JE007107

Mittelholz, A., Johnson, C. L., Feinberg, J. M., Langlais, B., & Phillips, R. J. (2020). Timing of the Martian dynamo: New constraints for a core field 4.5 and 3.7 Ga ago. *Science Advances, 6*, eaba0513. https://doi.org/10.1126/sciadv.aba0513

Molina-Cuberos, G. (2001). Cosmic ray and UV radiation models on the ancient Martian surface. *Icarus, 154*(1), 216–222. https://doi.org/10.1006/icar.2001.6658

Montabone, L., Spiga, A., Kass, D. M., Kleinböhl, A., Forget, F., & Millour, E. (2020). Martian Year 34 column dust climatology from mars climate sounder observations: Reconstructed maps and model simulations. *Journal of Geophysical Research: Planets, 125*(8), e2019JE006111.

Morris, R. V., Klingelhöfer, G., Schröder, C., Rodionov, D. S., Yen, A., Ming, D. W., De Souza, P. A., et al. (2006). Mössbauer mineralogy of rock, soil, and dust at Gusev Crater, Mars: Spirit's journey through weakly altered olivine basalt on the plains and pervasively altered basalt in the Columbia Hills. *Journal of Geophysical Research: Planets, 111*(E2), 2005JE002584. https://doi.org/10.1029/2005JE002584

Mumma, M. J., Villanueva, G. L., Novak, R. E., Hewagama, T., Bonev, B. P., DiSanti, M. A., Mandell, A. M., & Smith, M. D. (2009). Strong release of methane on Mars in Northern Summer 2003. *Science, 323*(5917), 1041–1045. https://doi.org/10.1126/science.1165243

Mustard, J. F., Poulet, F., Gendrin, A., Bibring, J.-P., Langevin, Y., Gondet, B., Mangold, N., Bellucci, G., & Altieri, F. (2005). Olivine and pyroxene diversity in the crust of Mars. *Science, 307*(5715), 1594–1597. https://doi.org/10.1126/science.1109098

Mustard, J. F. (2019). Sequestration of volatiles in the Martian crust through hydrated minerals. In *Volatiles in the Martian Crust* (pp. 247–263). Elsevier. https://doi.org/10.1016/B978-0-12-804191-8.00008-8

'NASA Astrobiology'. (2023, December 19). https://astrobiology.nasa.gov/news/water-on-mars-the-story-so-far/

Nesvorný, D., Janches, D., Vokrouhlický, D., Pokorný, P., Bottke, W. F., & Jenniskens, P. (2011). DYNAMICAL MODEL FOR THE ZODIACAL CLOUD AND SPORADIC METEORS. *The Astrophysical Journal, 743*(2), 129. https://doi.org/10.1088/0004-637X/743/2/129

Neukum, G., & Hiller, K. (1981). Martian ages. *Journal of Geophysical Research: Solid Earth, 86*(B4), 3097–3121. https://doi.org/10.1029/JB086iB04p03097

Neukum, G., Jaumann, R., Hoffmann, H., Hauber, E., Head, J. W., Basilevsky, A. T., Ivanov, B. A., Werner, S. C., & HRSC Co-investigator Team. (2004). Recent and episodic volcanic and glacial activity on Mars revealed by the high resolution stereo camera. *Nature, 432*, 971–979. https://doi.org/10.1038/nature03231

Nimmo, F. (2000). Dike intrusion as a possible cause of linear Martian magnetic anomalies. *Geology, 28*(5), 391–394. https://doi.org/10.1002/2013JE004499

Nimmo, F., & Faul, U. H. (2013). Dissipation at tidal and seismic frequencies in a melt-free, anhydrous Mars. *Journal of Geophysical Research (Planets), 118*, 2558–2569. https://doi.org/10.1002/2013JE004499

Nixon, S. L., Cousins, C. R., & Cockell, C. S. (2013). Plausible microbial metabolisms on Mars. *Astronomy & Geophysics, 54*(1), 1.13-1.16. https://doi.org/10.1093/astrogeo/ats034

Pál, B., Kereszturi, Á., Forget, F., & Smith, M. D. (2019). Global seasonal variations of the near-surface relative humidity levels on present-day Mars. *Icarus, 333*(November), 481–495. https://doi.org/10.1016/j.icarus.2019.07.007

Parenti, C., Gutiérrez, F., Baioni, D., García-Arnay, Á., Sevil, J., & Luzzi, E. (2020). Closed depressions in Kotido Crater, Arabia Terra, Mars. Possible evidence of evaporite dissolution-induced subsidence. *Icarus, 341*(May), 113680. https://doi.org/10.1016/j.icarus.2020.113680

Patel, M. R., Zarnecki, J. C., & Catling, D. C. (2002). Ultraviolet radiation on the surface of Mars and the Beagle 2 UV sensor. *Planetary and Space Science, 50*(9), 915–927. https://doi.org/10.1016/S0032-0633(02)00067-3

Pavlov, A. A., Vasilyev, G., Ostryakov, V. M., Pavlov, A. K., & Mahaffy, P. (2012). Degradation of the organic molecules in the shallow subsurface of Mars due to irradiation by cosmic rays. *Geophysical Research Letters, 39*(13), 2012GL052166. https://doi.org/10.1029/2012GL052166

Pavlov, A. A., McLain, H. L., Glavin, D. P., Roussel, A., Dworkin, J. P., Elsila, J. E., & Yocum, K. M. (2022). Rapid radiolytic degradation of amino acids in the Martian shallow subsurface: Implications for the search for extinct life. *Astrobiology, 22*(9), 1099–1115. https://doi.org/10.1089/ast.2021.0166

Payré, V., Fabre, C., Sautter, V., Cousin, A., Mangold, N., Le Deit, L., Forni, O., et al. (2019). Copper enrichments in the Kimberley formation in Gale Crater, Mars: Evidence for a Cu deposit at the source. *Icarus, 321*(March), 736–751. https://doi.org/10.1016/j.icarus.2018.12.015

Plesa, A. C., Tosi, N., & Breuer, D. (2014). Can a fractionally crystallized Magma Ocean explain the thermo-chemical evolution of Mars? *Earth and Planetary Science Letters, 403*, 225–235. https://doi.org/10.1016/j.epsl.2014.06.034

Plesa, A. C., Wieczorek, M. A., Knapmeyer, M., Rivoldini, A., Walterová, M., & Breuer, D. (2022). Interior dynamics and thermal evolution of Mars – a geodynamic perspective. In C. Schmelzbach & S. C. Stähler (Eds.), *Geophysical exploration of the solar system* (Vol. 63, pp. 179–230). Elsevier.

Plis, E. A., Engelhart, D. P., Russell Cooper, W., Johnston, R., Ferguson, D., & Hoffmann, R. (2019). Review of radiation-induced effects in polyimide. *Applied Sciences, 9*(10), 1999. https://doi.org/10.3390/app9101999

Poch, O., Kaci, S., Stalport, F., Szopa, C., & Coll, P. (2014). Laboratory insights into the chemical and kinetic evolution of several organic molecules under simulated Mars surface UV radiation conditions. *Icarus, 242*(November), 50–63. https://doi.org/10.1016/j.icarus.2014.07.014

Rafkin, S. C. R., Hollingsworth, J. L., Mischna, M. A., Newman, C. E., & Richardson, M. I. (2013). Mars: Atmosphere and climate overview. In *Comparative climatology of terrestrial planets*. University of Arizona Press. https://doi.org/10.2458/azu_uapress_9780816530595-ch003

Rampe, E. B., Bristow, T. F., Morris, R. V., Morrison, S. M., Achilles, C. N., Ming, D. W., Vaniman, D. T., et al. (2020a). Mineralogy of Vera Rubin ridge from the Mars science laboratory CheMin instrument. *Journal of Geophysical Research: Planets, 125*(9), e2019JE006306. https://doi.org/10.1029/2019JE006306

Rampe, E. B., Blake, D. F., Bristow, T. F., Ming, D. W., Vaniman, D. T., Morris, R. V., Achilles, C. N., et al. (2020b). Mineralogy and geochemistry of sedimentary rocks and Eolian sediments

in Gale Crater, Mars: A review after six earth years of exploration with Curiosity. *Geochemistry, 80*(2), 125605. https://doi.org/10.1016/j.chemer.2020.125605

Rampe, E. B., Ming, D. W., Blake, D. F., Bristow, T. F., Chipera, S. J., Grotzinger, J. P., Morris, R. V., et al. (2017). Mineralogy of an ancient lacustrine mudstone succession from the murray formation, Gale Crater, Mars. *Earth and Planetary Science Letters, 471*(August), 172–185. https://doi.org/10.1016/j.epsl.2017.04.021

Ramstad, R., Brain, D. A., Dong, Y., et al. (2020). The global current systems of the Martian induced magnetosphere. *Nature Astronomy, 4*, 979–985. https://doi.org/10.1038/s41550-020-1099-y

Reche, I., D'Orta, G., Mladenov, N., Winget, D. M., & Suttle, C. A. (2018). Deposition rates of viruses and bacteria above the atmospheric boundary layer. *The ISME Journal, 12*(4), 1154–1162. https://doi.org/10.1038/s41396-017-0042-4

Roberts, J. H., & Zhong, S. (2006). Degree-1 convection in the Martian mantle and the origin of the hemispheric dichotomy. *Journal of Geophysical Research (Planets), 111*, E06013. https://doi.org/10.1029/2005JE002668

Rodriguez, J. A., Dobrea, E. N., Kargel, J. S., Baker, V. R., Crown, D. A., Webster, K. D., Berman, D. C., Wilhelm, M. B., & Buckner, D. (2020). The oldest highlands of Mars may be massive dust fallout deposits. *Scientific Reports, 10*(1), 10347. https://doi.org/10.1038/s41598-020-64676-z

Rontó, G., Bérces, A., Lammer, H., Cockell, C. S., Molina-Cuberos, G. J., Patel, M. R., & Selsis, F. (2003). Solar UV irradiation conditions on the surface of Mars. *Photochemistry and Photobiology, 77*(1), 34–40. https://doi.org/10.1562/0031-8655(2003)0770034SUICOT2.0.CO2

Rubin, A. E., & Grossman, J. N. (2010). Meteorite and meteoroid: New comprehensive definitions. *Meteoritics and Planetary Science, February*. https://doi.org/10.1111/j.1945-5100.2009.01009.x

Salese, F., Di Achille, G., Neesemann, A., Ori, G. G., & Hauber, E. (2016). Hydrological and sedimentary analyses of well-preserved paleofluvial-paleolacustrine systems at Moa Valles, Mars. *Journal of Geophysical Research: Planets, 121*(2), 194–232. https://doi.org/10.1002/2015JE004891

Samuel, H., Drilleau, M., Garcia, R., Huang, Q., Rivoldini, A., Lognonné, P., & Banerdt, W. B. (2022). Testing the presence deep Martian mantle layering in the light of InSight seismic data. *Proceedings of the Europlanet Science Congress 2022*, EPSC Abstracts, 16:EPSC2022-297. https://doi.org/10.5194/epsc2022-297.

Samuel, H., Lognonné, P., Panning, M., et al. (2019). The rheology and thermal history of Mars revealed by the orbital evolution of Phobos. *Nature, 569*, 523–527. https://doi.org/10.1038/s41586-019-1202-7

Samuel, H., Drilleau, M., Rivoldini, A., Zongbo, X., Huang, Q., Garcia, R. F., Lekić, V., et al. (2023). Geophysical evidence for an enriched molten silicate layer above Mars's core. *Nature, 622*(7984), 712–717. https://doi.org/10.1038/s41586-023-06601-8

Sauterey, B., Charnay, B., Affholder, A., Mazevet, S., & Ferrière, R. (2022). Early Mars habitability and global cooling by H2-based methanogens. *Nature Astronomy, 6*(11), 1263–1271. https://doi.org/10.1038/s41550-022-01786-w

Sautter, V., Fabre, C., Forni, O., Toplis, M. J., Cousin, A., Ollila, A. M., Meslin, P. Y., et al. (2014). Igneous mineralogy at Bradbury rise: The first ChemCam campaign at Gale Crater. *Journal of Geophysical Research: Planets, 119*(1), 30–46. https://doi.org/10.1002/2013JE004472

Sautter, V., Toplis, M. J., Wiens, R. C., Cousin, A., Fabre, C., Gasnault, O., Maurice, S., et al. (2015). In situ evidence for continental crust on early Mars. *Nature Geoscience, 8*(8), 605–609. https://doi.org/10.1038/ngeo2474

Scheller, E. L., Ehlmann, B. L., Renyu, H., Adams, D. J., & Yung, Y. L. (2021). Long-term drying of Mars by sequestration of ocean-scale volumes of water in the crust. *Science, 372*(6537), 56–62. https://doi.org/10.1126/science.abc7717

Scheller, E. L., Bosak, T., McCubbin, F. M., Williford, K., Siljeström, S., Jakubek, R. S., Eckley, S. A., Morris, R. V., Bykov, S. V., Kizovski, T., Asher, S., Berger, E., Bower, D. M., Cardarelli, E. L., Ehlmann, B. L., Fornaro, T., Fox, A., Haney, N., Hand, K., Roppel, R., Sharma, S.,

Steele, A., Uckert, K., Yanchilina, A. G., Beyssac, O., Farley, K. A., Henneke, J., Heirwegh, C., Pedersen, D. A. K., Liu, Y., Schmidt, M. E., Sephton, M., Shuster, D., & Weiss, B. P. (2024). Inorganic interpretation of luminescent materials encountered by the perseverance rover on mars. *Science Advances, 10*(39), eadm8241.

Scheller, E. L., Hollis, J. R., Cardarelli, E. L., Steele, A., Beegle, L. W., Bhartia, R., Conrad, P., et al. (2022). Aqueous alteration processes in Jezero Crater, Mars—Implications for organic geochemistry. *Science, 378*(6624), 1105–1110. https://doi.org/10.1126/science.abo5204

Schmidt, M. E., Campbell, J. L., Gellert, R., Perrett, G. M., Treiman, A. H., Blaney, D. L., Olilla, A., et al. (2014). Geochemical diversity in first rocks examined by the Curiosity Rover in Gale Crater: Evidence for and significance of an alkali and volatile-rich igneous source. *Journal of Geophysical Research: Planets, 119*(1), 64–81. https://doi.org/10.1002/2013JE004481

Scott, D. H., & Carr, M. H. (1978). Geologic map of Mars. 1083. U.S. Geological Survey. https://doi.org/10.3133/i1083.

Sharma, S., Roppel, R. D., Murphy, A. E., Beegle, L. W., Bhartia, R., Steele, A., Hollis, J. R., et al. (2023). Diverse organic-mineral associations in Jezero Crater, Mars. *Nature, 619*(7971), 724–732. https://doi.org/10.1038/s41586-023-06143-z

Siljeström, S., Czaja, A. D., Corpolongo, A., Berger, E. L., Li, A. Y., Cardarelli, E., Abbey, W., et al. (2024). Evidence of sulfate-rich fluid alteration in Jezero Crater Floor, Mars. *Journal of Geophysical Research: Planets, 129*(1), e2023JE007989. https://doi.org/10.1029/2023JE007989

Simon, J. I., Hickman-Lewis, K., Cohen, B. A., Mayhew, L. E., Shuster, D. L., Debaille, V., Hausrath, E. M., et al. (2023). Samples collected from the floor of Jezero Crater with the Mars 2020 perseverance rover. *Journal of Geophysical Research: Planets, 128*(6), e2022JE007474. https://doi.org/10.1029/2022JE007474

Simpson, J. A. (1983). Elemental and isotopic composition of the galactic cosmic rays. *Annual Review of Nuclear and Particle Science, 33*(1), 323–382. https://doi.org/10.1146/annurev.ns.33.120183.001543

Smirnov, V. M., Semenov, A. S., Sokolov, V. G., Konoshenko, V. P., & Kovalyov, I. I. (2000). Study of micrometeoroid and orbital debris effects on the solar panels retrieved from the space station "MIR". *Space Debris, 2*(1), 1–7. https://doi.org/10.1023/A:1015607813420

Smith, K. C. (2009). The Trouble with intrinsic value: An ethical primer for astrobiology. In C. M. Bertka (Ed.), *Exploring the Origin, Extent, and Future of Life* (1st ed., pp. 261–280). Cambridge University Press. https://doi.org/10.1017/CBO9780511806506.014

Smith, P. H., Tamppari, L. K., Arvidson, R. E., Bass, D., Blaney, D., Boynton, W. V., Carswell, A., et al. (2009). H_2O at the Phoenix landing site. *Science, 325*(5936), 58–61. https://doi.org/10.1126/science.1172339

Squyres, S. W., & Carr, M. H. (1986). Geomorphic evidence for the distribution of ground ice on Mars. *Science, 231*(4735), 249–252. https://doi.org/10.1126/science.231.4735.249

Squyres, S. W., & Knoll, A. H. (2005). Sedimentary rocks at Meridiani Planum: Origin, diagenesis, and implications for life on Mars. *Earth and Planetary Science Letters, 240*(1), 1–10. https://doi.org/10.1016/j.epsl.2005.09.038

Stähler, S. C., Khan, A., Banerdt, W. B., Lognonné, P., Giardini, D., Ceylan, S., Drilleau, M., et al. (2021). Seismic detection of the Martian core. *Science, 373*(6553), 443–448. https://doi.org/10.1126/science.abi7730

Stalport, F., Coll, P., Szopa, C., Cottin, H., & Raulin, F. (2009). Investigating the photostability of carboxylic acids exposed to Mars surface ultraviolet radiation conditions. *Astrobiology, 9*(6), 543–549. https://doi.org/10.1089/ast.2008.0300

Stamenkovic, V., & Breuer, D. (2014). The tectonic mode of rocky planets: Part 1 – Driving factors, models & parameters. *Icarus, 234*, 174–193. https://doi.org/10.1016/j.icarus.2014.01.042

Stern, J. C., Sutter, B., Freissinet, C., Navarro-González, R., McKay, C. P., Douglas Archer, P., Buch, A., et al. (2015). Evidence for indigenous nitrogen in sedimentary and aeolian deposits from the *Curiosity* rover investigations at Gale Crater, Mars. *Proceedings of the National Academy of Sciences, 112*(14), 4245–4250. https://doi.org/10.1073/pnas.1420932112

Stuurman, C. M., Osinski, G. R., Holt, J. W., Levy, J. S., Brothers, T. C., Kerrigan, M., & Campbell, B. A. (2016). SHARAD detection and characterization of subsurface water ice deposits in Utopia Planitia, Mars. *Geophysical Research Letters, 43*(18), 9484–9491. https://doi.org/10.1002/2016GL070138

Sutter, B., McAdam, A. C., Mahaffy, P. R., Ming, D. W., Edgett, K. S., Rampe, E. B., Eigenbrode, J. L., et al. (2017). Evolved gas analyses of sedimentary rocks and Eolian sediment in Gale Crater, Mars: Results of the Curiosity Rover's sample analysis at Mars instrument from Yellowknife Bay to the Namib Dune. *Journal of Geophysical Research: Planets, 122*(12), 2574–2609. https://doi.org/10.1002/2016JE005225

Suzuki, Y., Trembath-Reichert, E., & Drake, H. (2022). Editorial: The rocky biosphere: New insights from microbiomes at rock-water interfaces and their interactions with minerals. *Frontiers in Microbiology, 13*(December), 1102710. https://doi.org/10.3389/fmicb.2022.1102710

Szopa, C., Freissinet, C., Glavin, D. P., Millan, M., Buch, A., Franz, H. B., Summons, R. E., et al. (2020). First detections of dichlorobenzene isomers and trichloromethylpropane from organic matter indigenous to Mars mudstone in Gale Crater, Mars: Results from the sample analysis at Mars instrument onboard the curiosity rover. *Astrobiology, 20*(2), 292–306. https://doi.org/10.1089/ast.2018.1908

Tanaka, K. L. (1986). The stratigraphy of Mars. *Journal of Geophysical Research: Solid Earth, 91*(B13). https://doi.org/10.1029/JB091iB13p0E139

Tanaka, K. L., Skinner, J. A., Jr., Dohm, J. M., Irwin, R. P., III, Kolb, E. J., Fortezzo, C. M., Platz, T., Michael, G. G., & Hare, T. M. (2014). *Geologic map of Mars: U.S. Geological Survey Scientific Investigations Map 3292*. Scientific Investigations Map.

The Omega Team, Poulet, F., Bibring, J.-P., Mustard, J. F., Gendrin, A., Mangold, N., Langevin, Y., Arvidson, R. E., Gondet, B., & Gomez, C. (2005). Phyllosilicates on Mars and implications for early Martian climate. *Nature, 438*(7068), 623–627. https://doi.org/10.1038/nature04274

Tomkins, A. G., Genge, M. J., Tait, A. W., Alkemade, S. L., Langendam, A. D., Perry, P. P., & Wilson, S. (2019). High survivability of micrometeorites on Mars: Sites with enhanced availability of limiting nutrients. *Journal of Geophysical Research: Planets, 124*(7), 1802–1818. https://doi.org/10.1029/2019JE006005

Vago, J. L., Westall, F., Coates, A. J., Jaumann, R., Korablev, O., Ciarletti, V., Mitrofanov, I., Josset, J.-L., De Sanctis, M. C., & Bibring, J.-P. (2017). Habitability on early Mars and the search for biosignatures with the ExoMars Rover. *Astrobiology, 17*(6-7), 471–510.

Vaniman, D. T., Martínez, G. M., Rampe, E. B., Bristow, T. F., Blake, D. F., Yen, A. S., Ming, D. W., et al. (2018). Gypsum, bassanite, and anhydrite at Gale Crater, Mars. *American Mineralogist, 103*(7), 1011–1020. https://doi.org/10.2138/am-2018-6346

Vicente-Retortillo, A., Martínez, G. M., Rennó, N. O., Lemmon, M. T., De La Torre-Juárez, M., & Gómez-Elvira, J. (2020). In situ UV measurements by MSL/REMS: Dust deposition and angular response corrections. *Space Science Reviews, 216*(5), 97. https://doi.org/10.1007/s11214-020-00722-6

Wang, A., Yan, Y., Jolliff, B. L., McLennan, S. M., Wang, K., Shi, E., & Farrell, W. M. (2020). Chlorine release from common chlorides by Martian dust activity. *Journal of Geophysical Research: Planets, 125*(6), e2019JE006283. https://doi.org/10.1029/2019JE006283

Wang, H., & Richardson, M. I. (2015). The origin, evolution, and trajectory of large dust storms on Mars during Mars years 24–30 (1999–2011). *Icarus, 251*(May), 112–127. https://doi.org/10.1016/j.icarus.2013.10.033

Watters, T. R., McGovern, P. J., & Irwin, R. P., III. (2007). Hemispheres apart: The crustal dichotomy on Mars. *Annual Review of Earth and Planetary Sciences, 35*(1), 621–652. https://doi.org/10.1146/annurev.earth.35.031306.140220

Way, M. J., Ostberg, C., Foley, B. J., Gillmann, C., Höning, D., Lammer, H., et al. (2023). Synergies between Venus & exoplanetary observations: Venus and its extrasolar siblings. *Space Science Reviews, 219*(1), 13. https://doi.org/10.1007/s11214-023-00953-3

Webster, C. R., Mahaffy, P. R., Atreya, S. K., Flesch, G. J., Mischna, M. A., Meslin, P.-Y., Farley, K. A., et al. (2015). Mars methane detection and variability at Gale Crater. *Science, 347*(6220), 415–417. https://doi.org/10.1126/science.1261713

Werner, S. C. (2019). In situ calibration of the Martian cratering chronology. *Meteoritics & Planetary Science, 54*(5), 1182–1193. https://doi.org/10.1111/maps.13263

Westall, F., Foucher, F., Bost, N., Bertrand, M., Loizeau, D., Vago, J. L., Kminek, G., et al. (2015). Biosignatures on Mars: What, where, and how? Implications for the search for Martian life. *Astrobiology, 15*(11), 998–1029. https://doi.org/10.1089/ast.2015.1374

Westall, F., Loizeau, D., Foucher, F., Bost, N., Betrand, M., Vago, J., & Kminek, G. (2013). Habitability on Mars from a microbial point of view. *Astrobiology, 13*(9), 887–897. https://doi.org/10.1089/ast.2013.1000

Wieczorek, M. A., Broquet, A., McLennan, S. M., Rivoldini, A., Golombek, M., Antonangeli, D., et al. (2022). InSight constraints on the global character of the Martian crust. *Journal of Geophysical Research (Planets), 127*, e2022JE007298. https://doi.org/10.1029/2022JE007298

Wieczorek, M. A., & Zuber, M. T. (2004). Thickness of the Martian crust: Improved constraints from geoid-to-topography ratios. *Journal of Geophysical Research (Planets), 109*(E1), E01009. https://doi.org/10.1029/2003JE002153

Wieczorek, M. A., Beuthe, M., Rivoldini, A., & Van Hoolst, T. (2019). Hydrostatic interfaces in bodies with nonhydrostatic lithospheres. *Journal of Geophysical Research: Planets, 124*(5), 1410–1432. https://doi.org/10.1029/2018JE005909

Wilson, J. T., Eke, V. R., Massey, R. J., Elphic, R. C., Feldman, W. C., Maurice, S., & Teodoro, L. F. A. (2018). Equatorial locations of water on Mars: Improved resolution maps based on Mars Odyssey neutron spectrometer data. *Icarus, 299*(January), 148–160. https://doi.org/10.1016/j.icarus.2017.07.028

Wilson, S. A., Howard, A. D., Moore, J. M., & Grant, J. A. (2016). A cold-wet middle-latitude environment on Mars during the Hesperian-Amazonian transition: Evidence from Northern Arabia Valleys and Paleolakes. *Journal of Geophysical Research: Planets, 121*(9), 1667–1694. https://doi.org/10.1002/2016JE005052

Wittmann, A., Korotev, R. L., Jolliff, B. L., Irving, A. J., Moser, D. E., Barker, I., & Rumble, D. (2015). Petrography and composition of Martian Regolith Breccia Meteorite Northwest Africa 7475. *Meteoritics & Planetary Science, 50*(2), 326–352. https://doi.org/10.1111/maps.12425

Wynne, J. J., Mylroie, J. E., Titus, T. N., Malaska, M. J., Buczkowski, D. L., Buhler, P. B., Byrne, P. K., Cushing, G. E., Davies, A. G., & Frumkin, A. (2022a). Planetary caves: A solar system view of processes and products. *Journal of Geophysical Research: Planets, 127*(11), e2022JE007303.

Wynne, J. J., Titus, T. N., Agha-Mohammadi, A.-a., Azua-Bustos, A., Boston, P. J., De León, P., Demirel-Floyd, C., et al. (2022b). Fundamental science and engineering questions in planetary cave exploration. *Journal of Geophysical Research: Planets, 127*(11), e2022JE007194. https://doi.org/10.1029/2022JE007194

Yoder, C. F., Konopliv, A. S., Yuan, D. N., Standish, E. M., & Folkner, W. M. (2003). Fluid core size of Mars from detection of the solar tide. *Science, 300*(5617), 299–303. https://doi.org/10.1126/science.1079645

Zhang, J., Guo, J., Dobynde, M. I., Wang, Y., & Wimmer-Schweingruber, R. F. (2022). From the top of Martian Olympus to deep craters and beneath: Mars radiation environment under different atmospheric and regolith depths. *Journal of Geophysical Research: Planets, 127*(3), e2021JE007157. https://doi.org/10.1029/2021JE007157

Zhong, S., & Zuber, M. T. (2001). Degree-1 mantle convection and the crustal dichotomy on Mars. *Earth and Planetary Science Letters, 189*, 75–84. https://doi.org/10.1029/2005JE002668